A Reference Field for GCR Simulation and an LET-Based Implementation at NSRL

T.C. Slaba[1], S.R. Blattnig[1], S.A. Walker[2], J.W. Norbury[1]

[1] NASA Langley Research Center, Hampton, VA
[2] Old Dominion University Research Foundation, Norfolk, VA

2015 HRP Investigators' Workshop
Jan 13-15, 2015
Galveston, TX

Outline

- Motivation
- External vs. internal (tissue) environments
- Variation in exposure quantities
  - Shielding configuration and solar activity
  - Identify reference field
- Sensitivity analyses
  - Which ions/energies are most important
  - Impact of energy constraints
- Beam selection strategy
- Discussion and summary

Motivation

- GCR simulator at NSRL is intended to deliver the ambient radiation field found in deep space in a controlled laboratory environment

- Simulator may be used to study the following areas in radiobiology
  - Long term and CNS effects in animal models
  - Dose rate effects
  - Mixed field effects (energy and particle type)
  - Countermeasures for chronic exposure

- First goal is to determine a reference field to use in such studies
  - Want investigators using a common reference field (for now) for consistency and possible cross-comparisons (also saves time and cost)

External and Internal Fields

- The external GCR field is modified as it passes through shielding and tissue
  - Slowing down due to atomic processes
  - Attenuation and breakup of heavy ions due to nuclear collisions
  - Secondary particle production
  - Plot below (right) for minimal shielding (5 g/cm^2) and average tissue (30 g/cm^2)

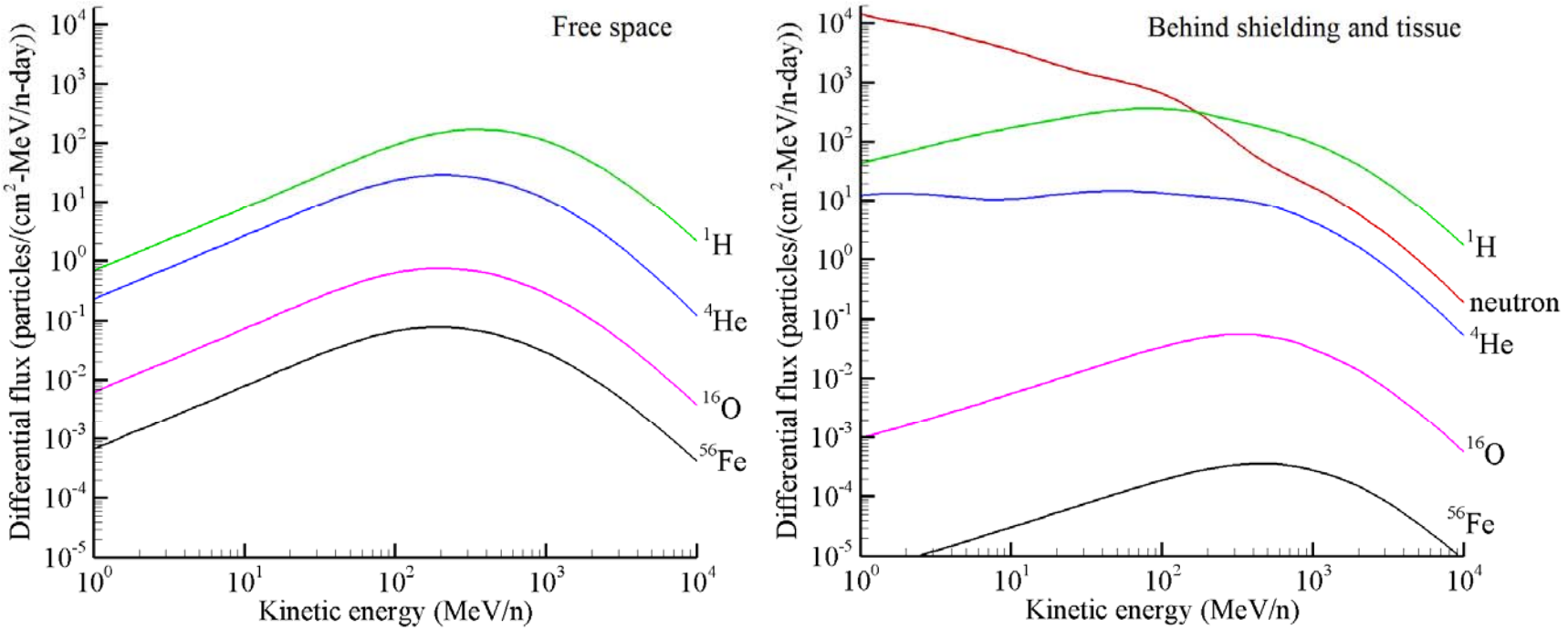

Selected particle spectra in free space (left pane) and behind 5 g/cm^2 of aluminum and 30 g/cm^2 of water (right pane) during solar minimum

External and Internal Fields

- An important question is whether to design the simulator using the free space, external field or local tissue field

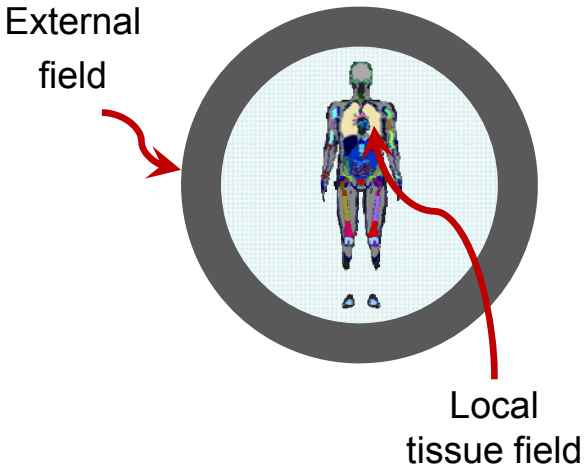

- External field approach:
  - Select ions and energies to represent external field
  - Place shielding in beam line in front of biological target
  - Beams fired onto target

- Local tissue field approach:
  - Use models to predict exposure quantities for local tissue field
  - Select ions and energies to represent local tissue field
  - Beams fired directly onto biological target

- Facility constraints play a significant role in this decision
  - Sensitivity studies carried out to determine which energies are most important in each scenario

External and Internal Fields

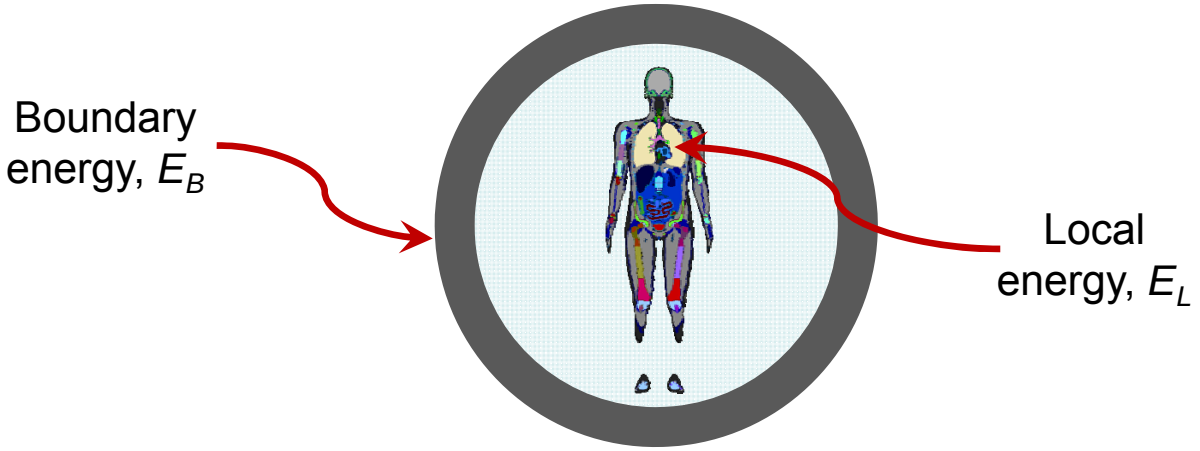

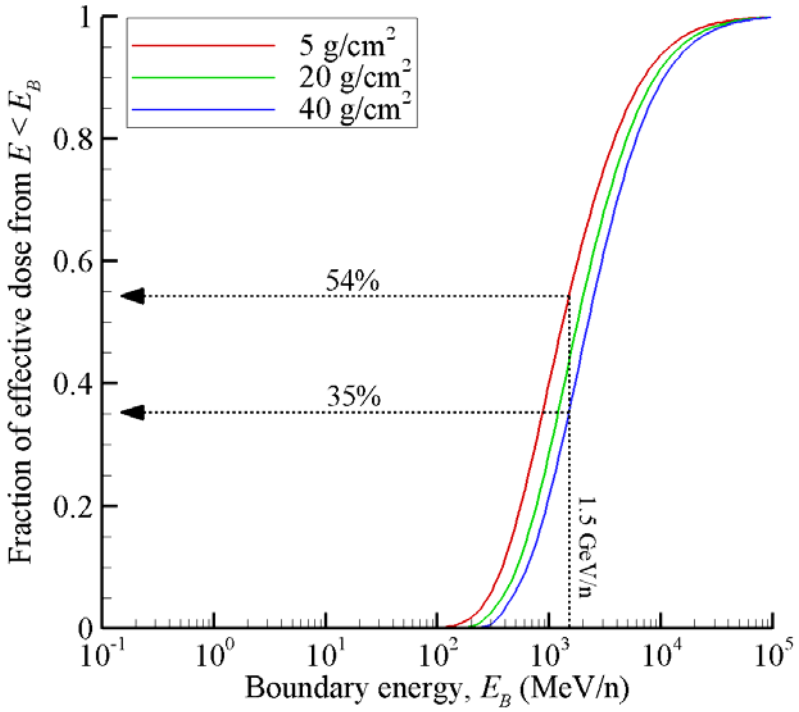

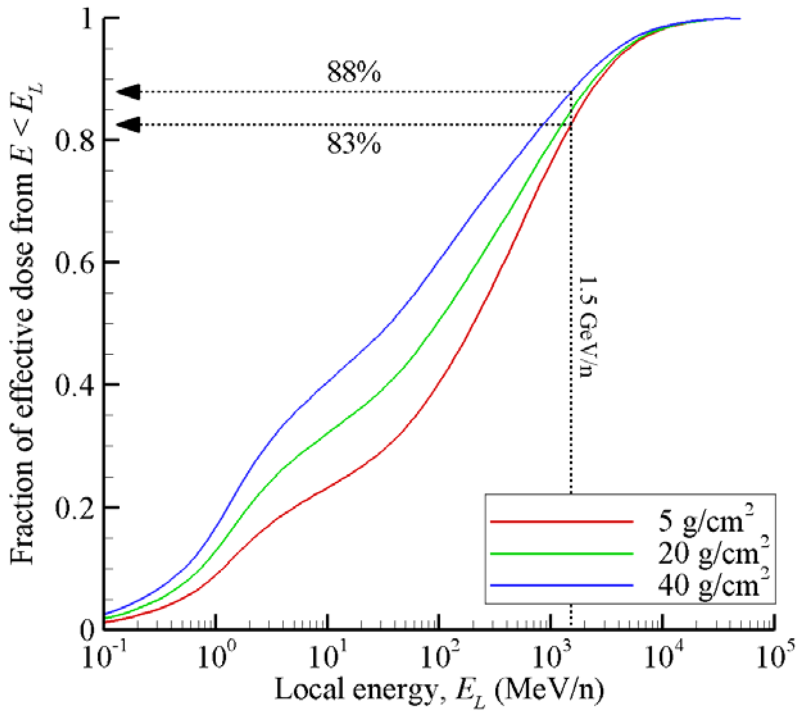

External and Internal Fields

- Plots below show fraction of effective dose as a function of boundary and local energies for thicknesses of aluminum shielding
  - Current NSRL constraints appear to be restrictive if external, free space field is simulated
  - Appears energy domain of local tissue field can be well represented

Simulator design related to external field

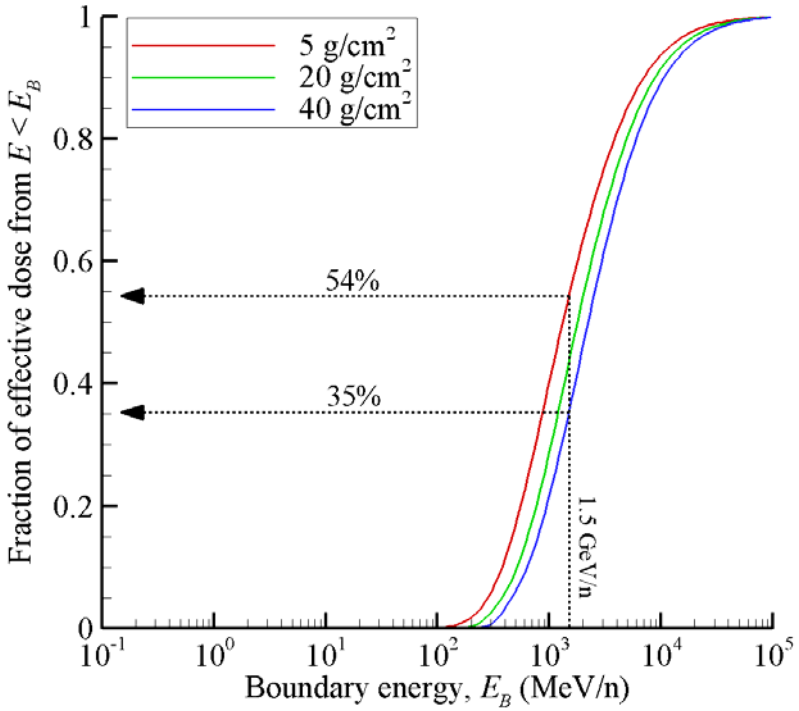

Simulator design related to local tissue field

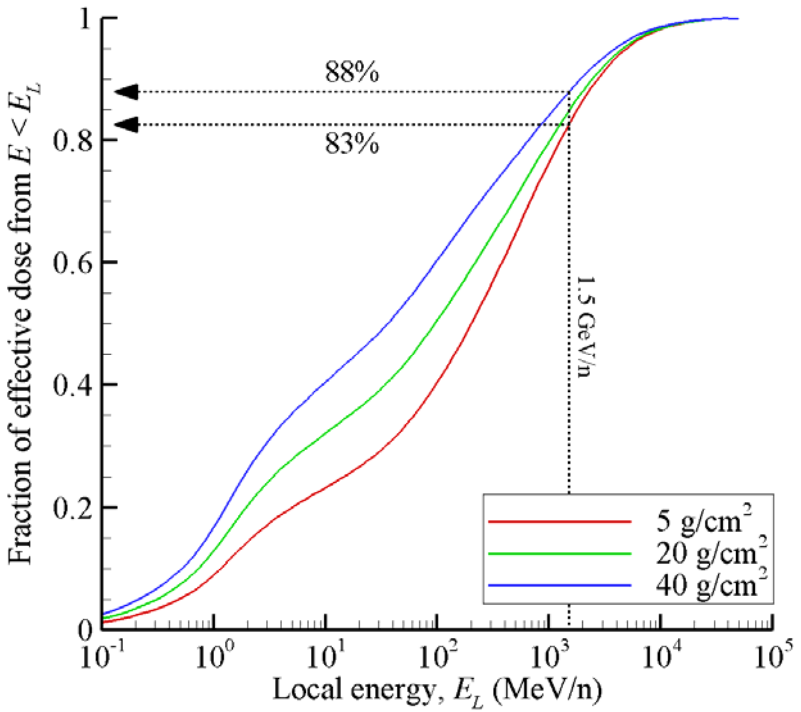

External and Internal Fields

- Table below gives fraction of effective dose delivered by energies within NSRL constraints (current and upgrade) behind aluminum shielding
  - Missing ~half of the exposure if free space field is simulated
  - Current (and upgraded) NSRL constraints provide good energy coverage of the local field
  - Need to determine whether NSRL constraints impose a qualitative problem (i.e. can beam intensities below cutoff just be increased to offset the problem)

Energy cutoff description	**Free space field**			**Local field**		
	5 g/cm^2	20 g/cm^2	40 g/cm^2	5 g/cm^2	20 g/cm^2	40 g/cm^2
Protons up to 2.5 GeV and heavier ions up to 1.0 GeV/n	0.53	0.47	0.43	0.85	0.88	0.90
Protons up to 4 GeV and heavier ions up to 1.5 GeV/n	0.68	0.63	0.59	0.90	0.91	0.93

External and Internal Fields

- Plots below compare LET spectra in female BFO behind 20 g/cm^2 aluminum shielding during solar minimum
  - Dashed black line obtained with full representation of GCR boundary condition
  - Red line obtained with cutoff GCR boundary condition: Current NSRL energy constraints applied

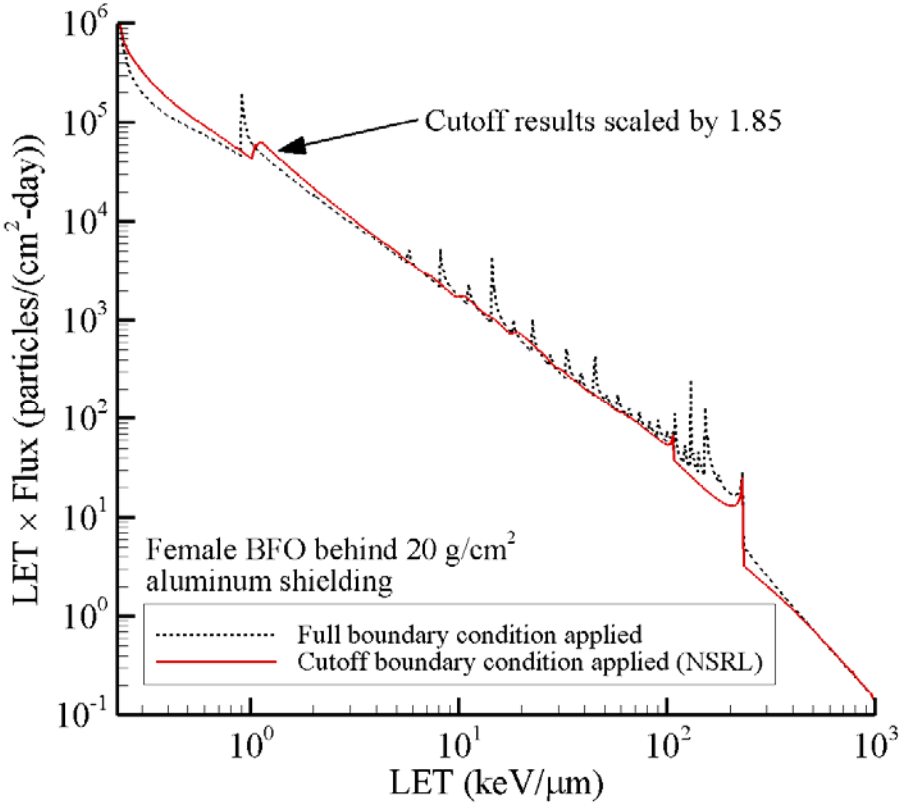

- Single scale factor of 1.85 provides reasonable qualitative agreement between results
  - Assumes that boundary condition below NSRL cutoff is fully represented, which is not realistic
  - If possible, decent representation of the full result can be obtained within NSRL energy constraints (only need to scale beam intensities up to match exposure quantities)

External and Internal Fields

- Possible beam selection strategy
  - One way to select beams in either approach is to bin the LET domain and represent each LET bin with a mono-energetic ion beam
  - Beam energies are bounded above by NSRL constraints
  - Beam energies are bounded below by shield/target configuration (want to avoid primary beams stopping in target to avoid rapid exposure gradients)
  - Optimization procedure for selecting beams against energy constraints is greatly complicated if external field is simulated

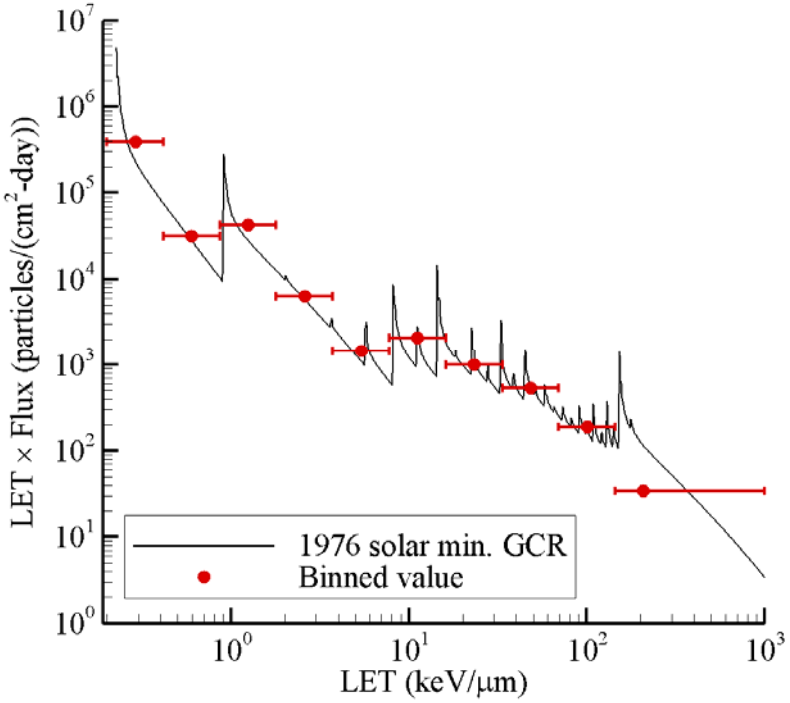

External and Internal Fields

- External field approach
  - Pros:
    - Broad spectrum of particles/energies will reach biological target due to fragmentation in shield
    - Neutrons will be generated in shield (small fraction of the π/EM cascade as well)
  - Cons:
    - Difficult to characterize exactly what impinges on biological target
    - Difficult to relate experimental results to single beam studies where beam is fired directly onto target
    - Energy constraints (lower and upper) complicate beam selection and related optimization strategies
    - Reproducibility becomes an issue for subsequent experiments
      - Statistical fluctuations due to nuclear interactions
      - Possible issue with exposure gradient with in animal

- Local tissue field approach
  - Pros:
    - Reproducibility in subsequent experiments
    - Field impinging on biological target is much easier to characterize and understand
    - Experimental results can be related to single beam studies more directly
  - Cons:
    - Neutrons and π/EM not well represented

Variation in Local Field

- The local tissue field varies with
  - tissue location within the body
  - shield configuration (geometry, thickness, material)
  - solar activity

- Intended usage of simulator helps focus and constrain variable space
  - Minimal shielding conditions associated with spacesuit/EVA less important
  - Increased skin exposure compared to other tissues less important
  - Vehicle shielding comprised of mostly aluminum

Variation in Local Field

- Need to determine if variation is significant enough to require multiple reference fields to be specified

- If variation is within physics uncertainties, radiobiology uncertainties, or uncertainties associated with experimental design, then multiple reference fields are not needed
  - Benefit to having a single field is that experiments will all have same exposure regimen
  - Improved value of subsequent cross-comparisons

- GCR environmental model uncertainty is at least ±20% [1]
- Combined environmental, physics, and transport uncertainty likely larger [2-4]
- Quality factor uncertainty is approximately 2.5 fold in NSCR2012 [5]
- Experimental design uncertainties not yet quantified
  - Error associated with representing full space environment with relatively few beams

Variation in Local Field

- Will consider spherical aluminum shielding (5 g/cm^2, 20 g/cm^2, 40 g/cm^2) along with four realistic shielding geometries
  - Habitat demonstration unit (HDU) adapted for 1-year free space mission [6]
  - Cislunar vehicle concept [7]
  - ISS location in US Lab near overhead racks
  - STS location in mid-deck (often referred to as DLOC 2)

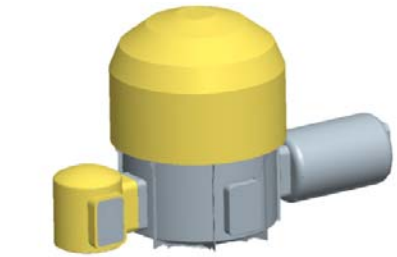
HDU

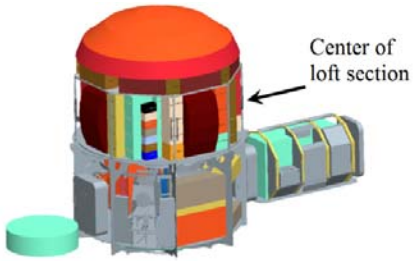

HDU without walls

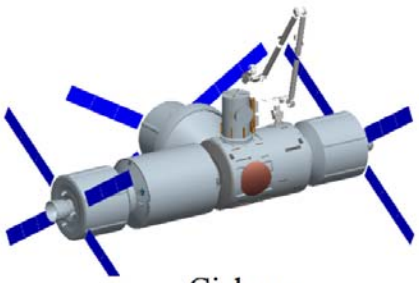
Cislunar

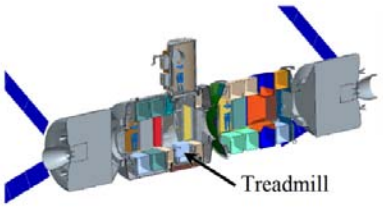

Cislunar cutaway

Variation in Local Field

- Variation in local tissue field will be examined as a function of
  - Tissue location
  - Shielding configuration
  - Shielding material
  - Solar activity

- Models
  - GCR environment computed with the 2010 Badhwar-O'Neill GCR model [8]
    - Solar minimum: June 1976
    - Solar maximum: June 2001
    - All results shown for solar minimum except for comparisons focused on solar activity
  - HZETRN transport code with π/EM and bi-directional neutron transport (ray-by-ray) [9-13, 2]
  - Female phantom (FAX) [14]
  - NASA - Q and effective dose tissue weights implemented where applicable [5]
  - Q-factor uncertainties from NSCR2012 implemented where applicable [5]

Variation in Local Field – Shielding

- Plots below show tissue doses and dose equivalents behind shielding
  - Variation is within even the GCR environmental model uncertainty (~±20%)
  - Increased variation in dose equivalent associated with HZE breakup
  - Bladder, BFO and breast appear as representative tissues
  - 20 g/cm^2 aluminum appears as representative shielding

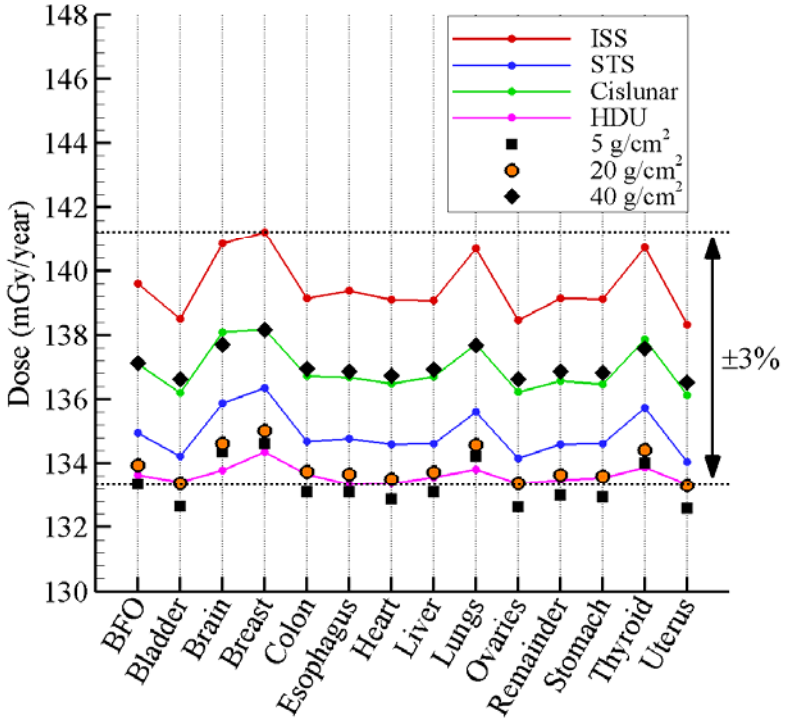

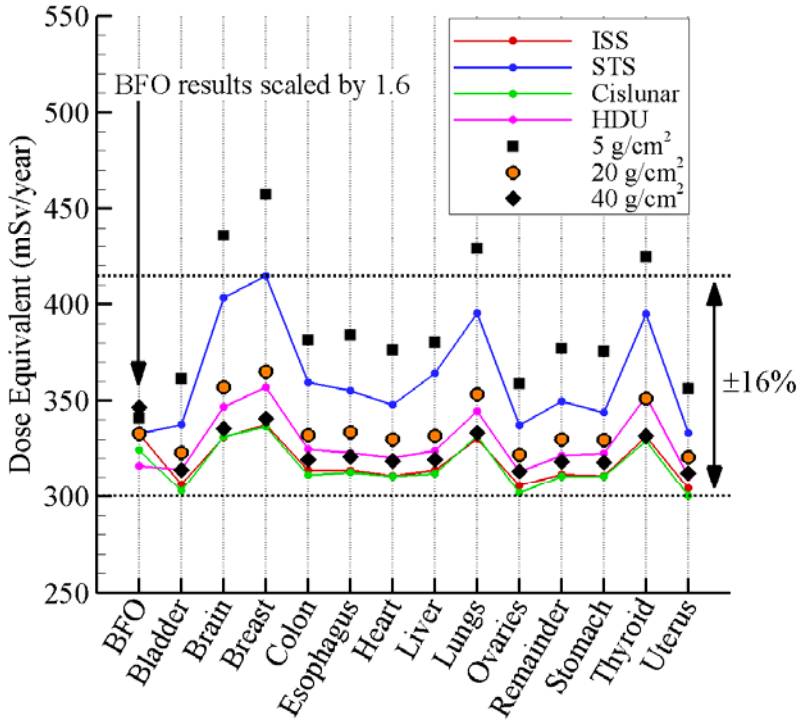

Variation in Local Field – Shielding

- LET spectral comparisons in different shielding configurations and tissues
  - Variation associated with shielding appears small below 200 keV/μm
  - Variation is within uncertainty associated with predicting such spectra [4, 15]
  - Spectra appear as qualitatively similar

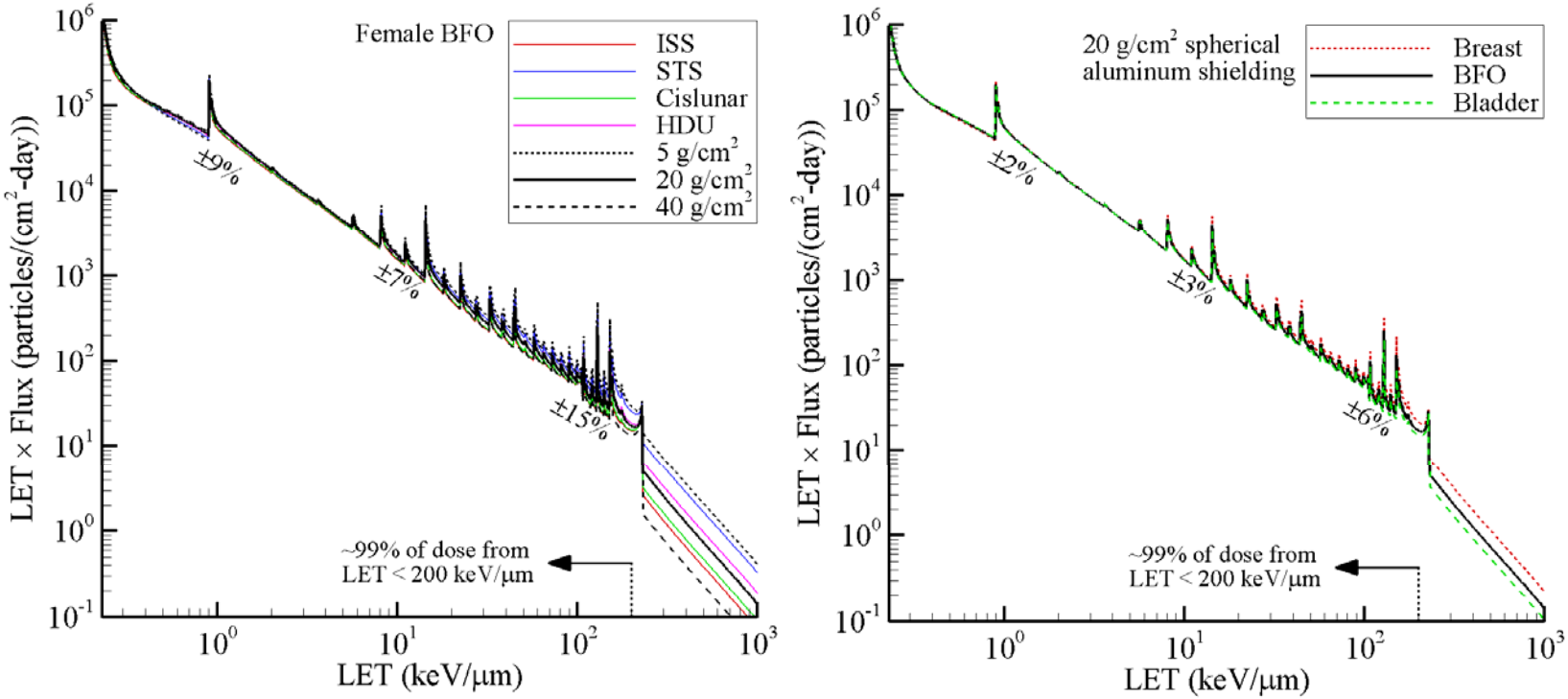

Variation in Local Field – Shielding

- Shielding material also contributes to variation in exposure quantities
  - Current technology suggests deep space vehicle will be comprised of mainly aluminum with some parasitic shielding mass (polyethylene)
  - Plot below shows tissue exposure values behind 20 g/cm^2 of aluminum or polyethylene
  - Variation is within environmental and physics modeling uncertainty

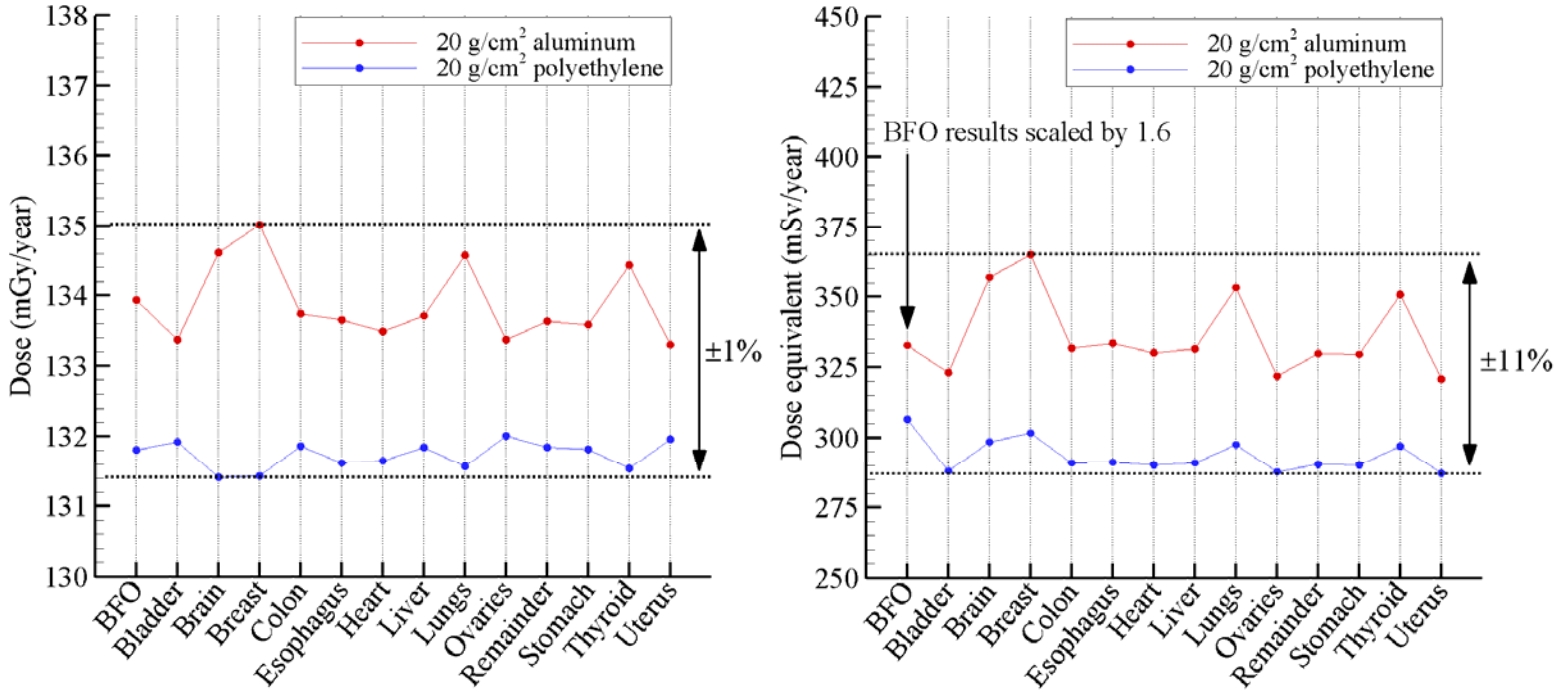

Variation in Local Field – Solar Activity

- During solar max, the GCR spectrum is attenuated below several GeV/n
  - Plots below compare solar minimum and solar maximum results
  - Solar maximum results have been scaled by 1.85
  - Constant factor of 1.85 nearly corrects discrepancies associated with solar activity across the entire LET domain
  - Suggests main difference between solar extremes is magnitude of exposure, not the shape of the LET spectrum

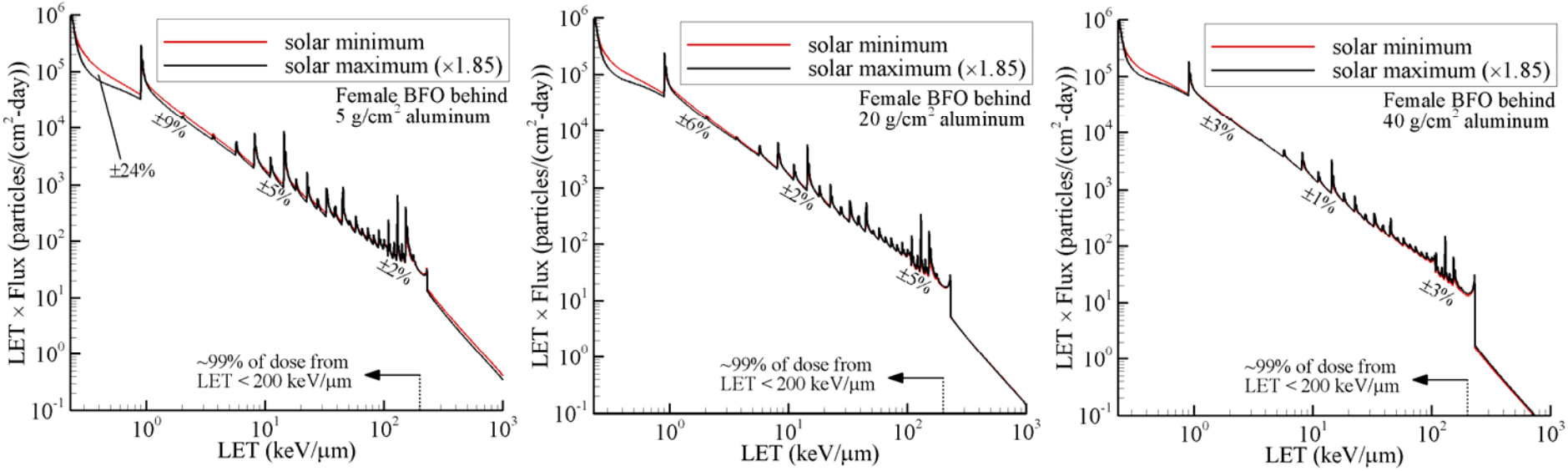

Variation in Local Field - Summary

- Variation associated with shielding configuration was considered
  - Observed differences were found to be within modeling uncertainty
  - LET spectra in various tissues and shielding configurations found to be qualitatively similar

- Variation associated with solar activity was examined
  - Observed differences could be approximately corrected with a single scale factor of 1.85
  - This indicates there is not a significant qualitative difference between solar extremes

- In general, the physics behind shielding/tissue is not greatly altered with any of the above conditions
  - Variation is well within current radiobiology uncertainties across LET spectrum
  - Variation is likely within uncertainty associated with simulator design

- It does not seem necessary to suggest/define several reference environments for various shielding and solar activity scenarios

Reference Field Specification

- Reference field is specified as the female BFO environment behind 20 g/cm^2 spherical aluminum shielding during solar minimum
  - BFO exposures found to be near average of all tissue results
  - 20 g/cm^2 aluminum shielding results fell within the bounds set by complicated geometries
  - Solar activity can be accounted for by scaling the total exposure up or down
  - LET spectrum of reference field shown along with dose and dose equivalent values

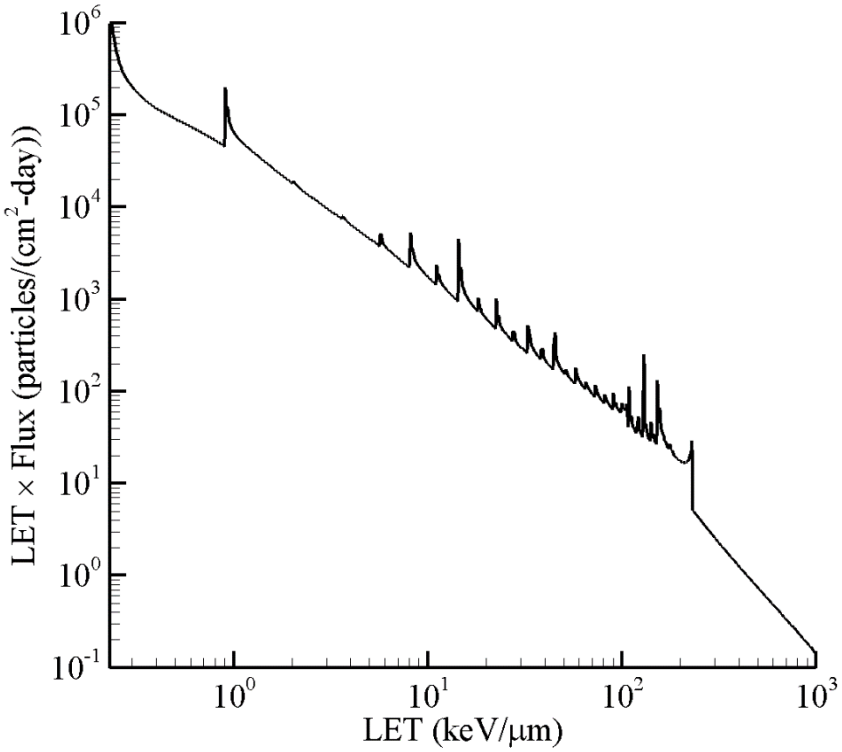

	D	H_{solid}	$<Q_{solid}>$
π/EM	15.5	15.5	1.0
neutron	1.1	22.9	20.4
proton	79.1	115.0	1.5
alpha	17.4	76.2	4.4
HZE	8.9	73.3	8.2
Total	133.9	336.6	2.5

Sensitivity Analysis

- Before developing procedures to simulate the designated reference field, it is helpful to look more carefully at particles and energies contributing to the local exposure
  - Helps guide discrete beam selection

- Have already shown that current NSRL upper energy limits are not restrictive for simulating local tissue field
  - Current constraints deliver 85% of the exposure
  - Upgrade constraints deliver 90% of the exposure

Sensitivity Analysis

- Plots below show relative contribution to dose and dose equivalent from various particles in the reference field
- Z = 1 and Z = 2 contributions dominate
  - 81% of dose and 67% of dose equivalent
- Z > 2 contributes 7% to dose and 21% to dose equivalent
  - Z = 6,7,8,10,12,14,20,26 appear amplified compared to other heavy ions

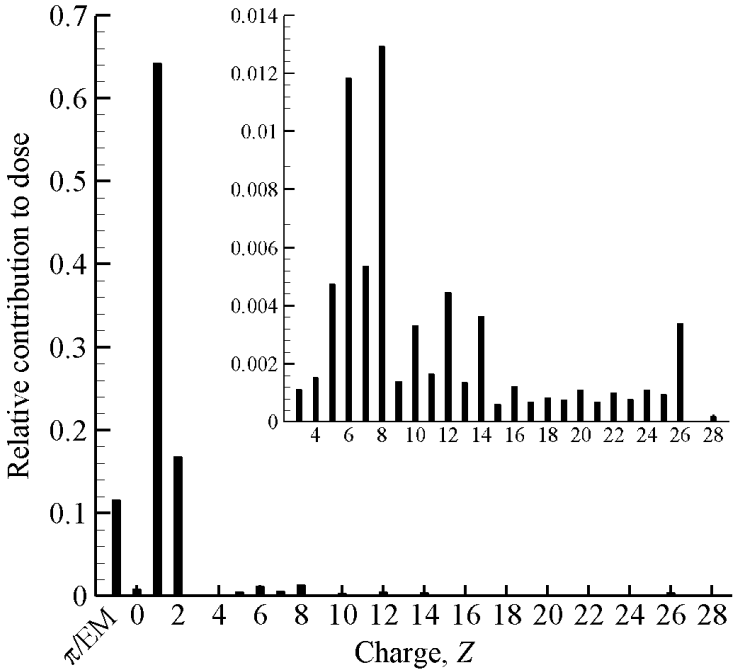

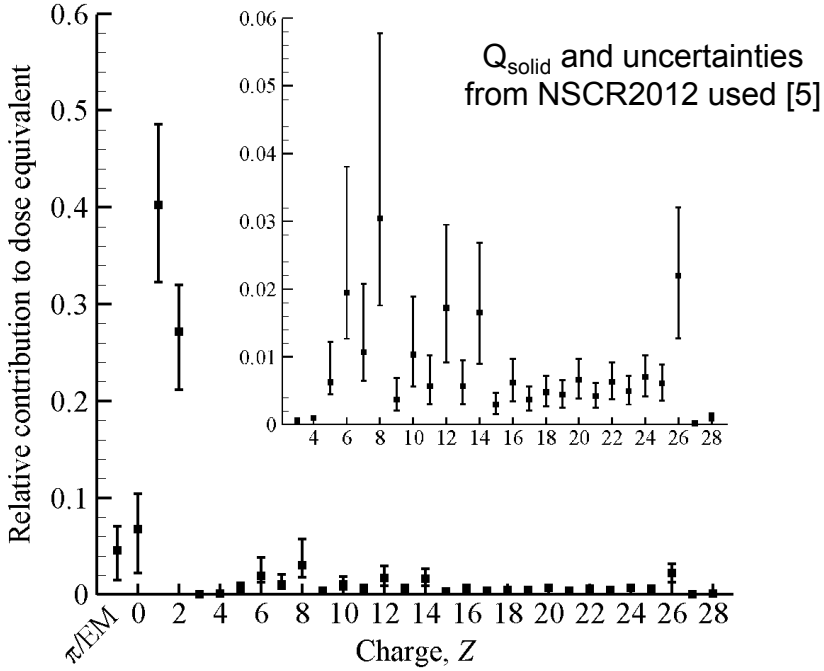

Sensitivity Analysis

- Another point to consider is the self-shielding provided by an animal model
  - May want to avoid Bragg peaks or rapid exposure gradients within mice
  - Localized tissue exposures may be difficult to reproduce in subsequent studies
  - Assume mouse is represented by cylindrical phantom (length 8 cm and radius 2.3 cm)
  - Table below gives energies needed to reach 9 cm

Z	E to reach 9 cm (MeV/n)	E to reach 80 cm (MeV/n)
1	109	393
2	109	393
6	204	806
7	224	898
8	242	987
10	277	1166
12	308	1336
14	339	1499
26	475	2334

Beam Specification Strategy

- Beam selection strategy guided primarily by LET spectrum of reference environment
  - Want to reproduce LET spectrum
  - This should closely reproduce reference dose, dose eq, and <Q> values
  - Can look at other quantities as independent check (track structure parameter spectrum)
  - Neutron and π/EM components not included in LET spectrum (discussed later)

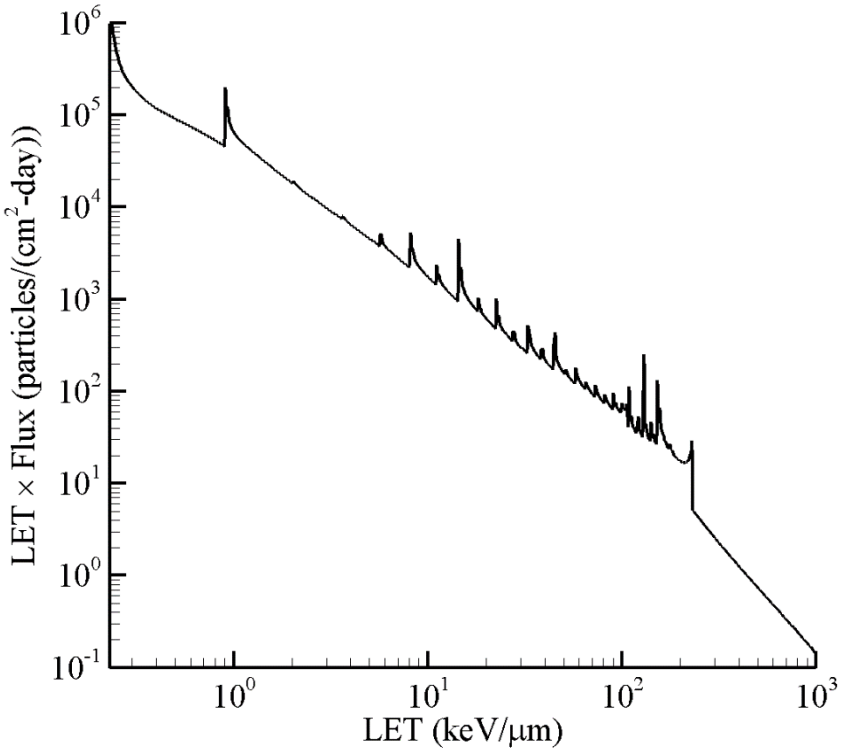

	D	H_{solid}	$<Q_{solid}>$
π/EM	15.5	15.5	1.0
neutron	1.1	22.9	20.4
proton	79.1	115.0	1.5
alpha	17.4	76.2	4.4
HZE	8.9	73.3	8.2
Total	133.9	336.6	2.5

Beam Specification Strategy

- Beam selection strategy guided primarily by LET spectrum of reference environment
  - Sensitivity results provide ancillary information

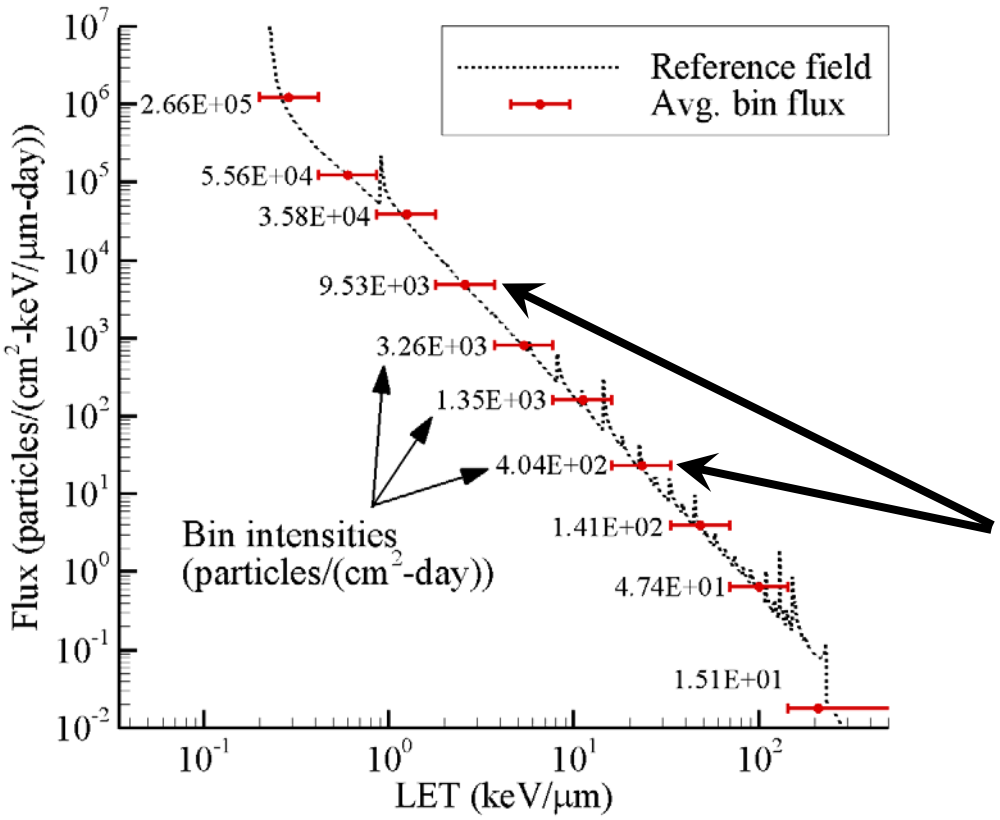

- LET domain is separated into uniformly spaced bins in log-space
  - 10 bins in this example
- Bin widths indicated by horizontal error bars

Beam Specification Strategy

- Beam selection strategy guided primarily by LET spectrum of reference environment
  - Sensitivity results provide ancillary information

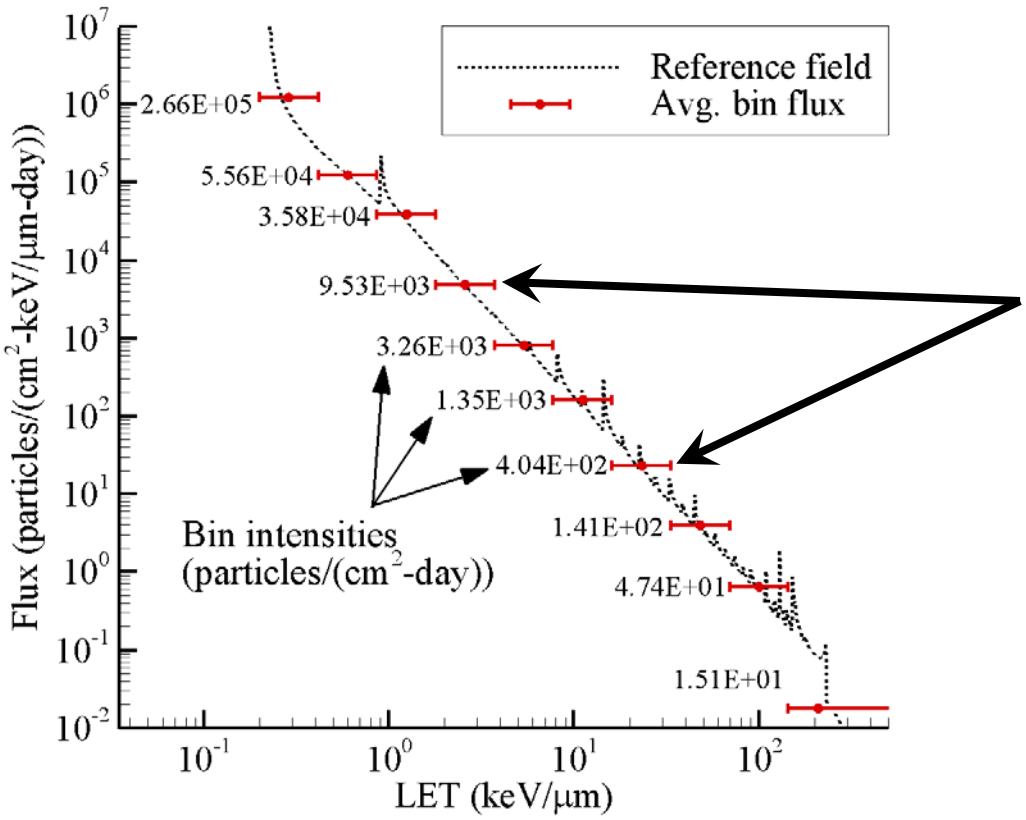

- Each bin represented by mono-energetic ion beam
- Beam intensity set by integrating reference field over bin width
- Intensities can be scaled up or down, but relative variation between bins needs to be maintained

Beam Specification Strategy

- Beam selection strategy guided primarily by LET spectrum of reference environment
  - Sensitivity results provide ancillary information

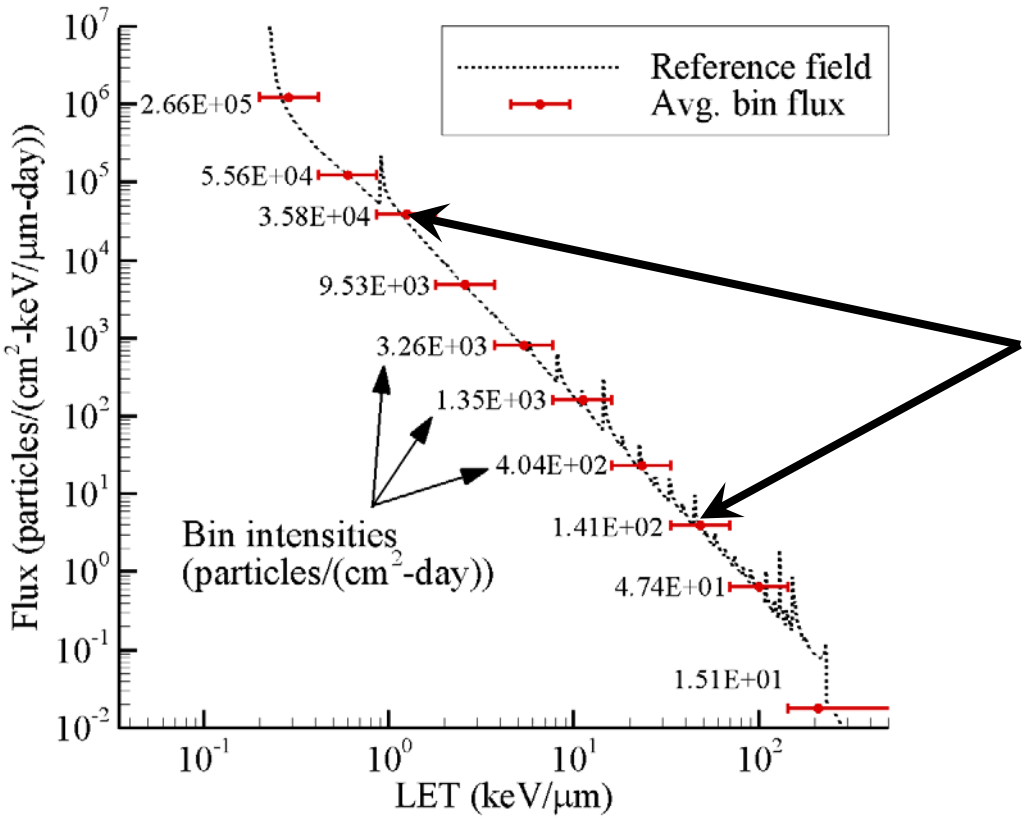

- The midpoint LET value of each bin will be used to select beam ions and energies
- Multiple ions with different energies may have same LET

Beam Specification Strategy

- Imposing energy constraints into the problem reduces the number of particles with the same LET
  - NSRL provides upper energy limitation
  - Animal model provides lower energy limitation
- Consider the bin at ~11 keV/μm
  - Only Z = 5, 6 have energies within energy constraints
  - Z=6 is chosen based on importance in sensitivity analysis
  - Similar analysis carried out for other bins

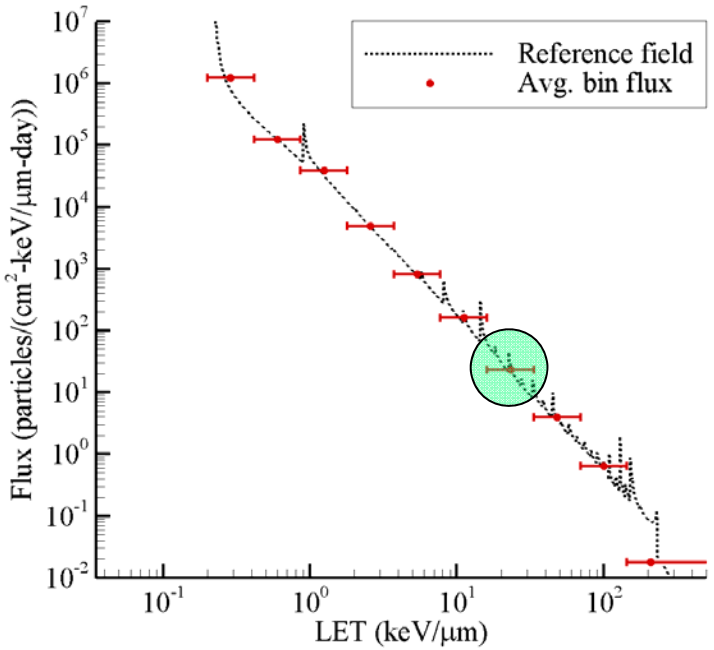

Ions and energies with LET of ~11 keV/μm

Charge, Z	Energy (MeV/n)
1	3.6
2	20.8
3	56.8
4	120.9
5	234.9
6	468.4
7	1590.0
7	3525.33

Beam Specification Strategy

- Final beam selection and related quantities for each bin is given below
- Subsequent analyses (using HZETRN for beam transport – see backup slides)
  - Consider how tissue shielding of animal alters primary beams
  - Compare LET spectra of beams to spectra at a point in phantom
  - Consider track structure parameter spectrum, $F[(Z^*/\beta)^2]$

A	Z	Energy (MeV/n)	LET (keV/μm)	$(Z^*/\beta)^2$	Intensity (# cm^{-2} day^{-1})	Dose (μGy/day)
1	1	560.0	0.29	1.64	2.66×10^5	111.4
1	1	150.0	0.60	3.90	5.56×10^4	48.5
4	2	464.9	1.25	7.23	3.58×10^4	64.9
4	2	134.5	2.59	17.02	9.53×10^3	35.9
7	3	150.7	5.37	34.94	3.26×10^3	25.5
12	6	468.4	11.17	64.85	1.35×10^3	22.0
16	8	338.8	23.20	139.08	4.04×10^2	13.7
28	14	948.0	48.21	260.44	1.41×10^2	9.9
40	20	877.6	100.16	545.70	4.74×10^1	6.9
56	26	476.4	208.12	1206.88	1.51×10^1	4.6
Totals					3.72×10^5	343.3

Beam Specification Strategy

- To examine variation within animal, consider a cylindrical water phantom randomly oriented in xy-plane using 1000 Monte Carlo trials

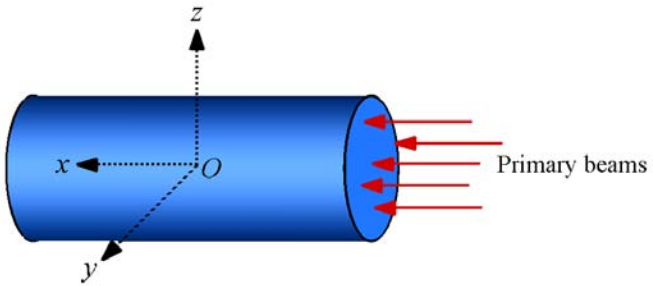

Rotations taken about
z-axis in *xy*-plane

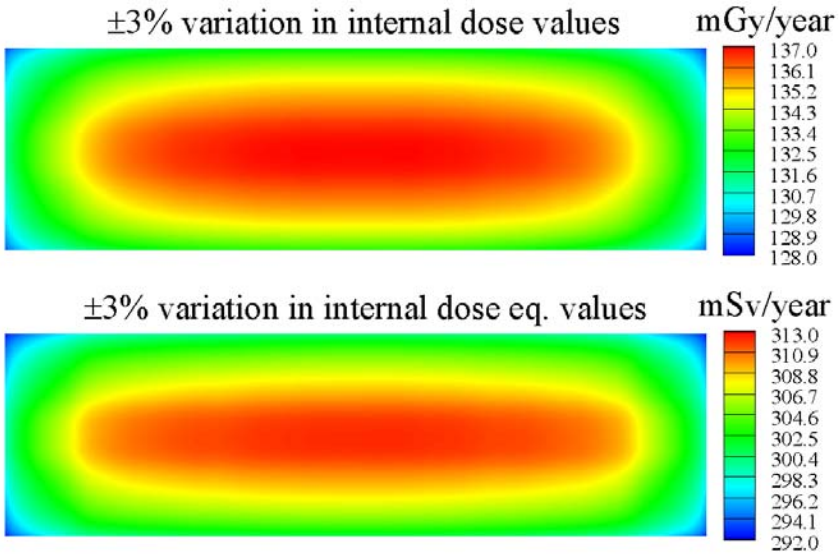

- Contour plots shown for xy-slice at z=0
- Exposure values show little variation within the phantom

Beam Specification Strategy

- Plot below compares LET spectra at boundary and at a point in the center of the phantom (random orientation again implemented)
  - Dose and dose equivalents at boundary and at center of phantom compared to reference values in table
  - Overall good agreement (even with 10 beams) in spectral and integrated quantities

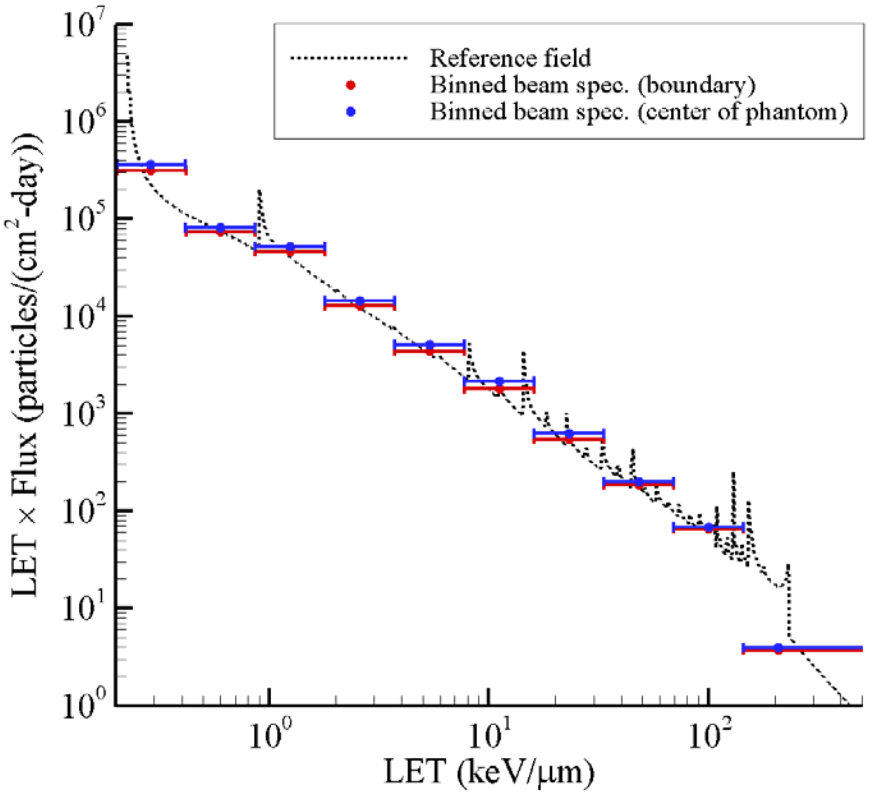

	D	H_{solid}	$\langle Q_{solid} \rangle$
Boundary	125.3	259.3	2.07
Center of phantom	140.2	318.5	2.27
Reference field (ions only)	117.3	298.2	2.54

Beam Specification Strategy

- Track structure parameter, $X_{tr} = (Z^*/\beta)^2$, has been presented as an improved descriptor of track structure effects compared to LET alone [5]
- Beam selection not guided by X_{tr} spectra, so $F(X_{tr})$ provides somewhat of an independent check

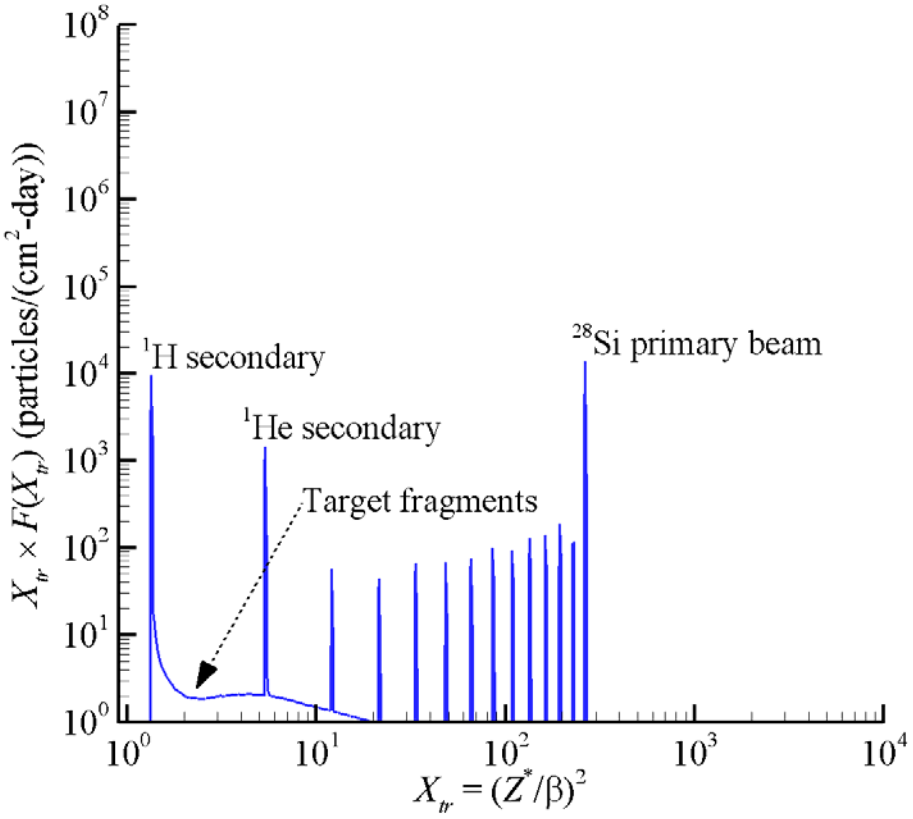

- Plot shows $F(X_{tr})$ at a point in the phantom exposed to just the ^{28}Si beam (948 MeV/n)
- Peaks at lower X_{tr} values correspond to heavy ion projectile fragments with similar velocity
- Target fragment spectrum can be seen as well

Beam Specification Strategy

- Track structure parameter, $X_{tr} = (Z^*/\beta)^2$, has been presented as an improved descriptor of track structure effects compared to LET alone [5]
- Beam selection not guided by X_{tr} spectra, so $F(X_{tr})$ provides somewhat of an independent check

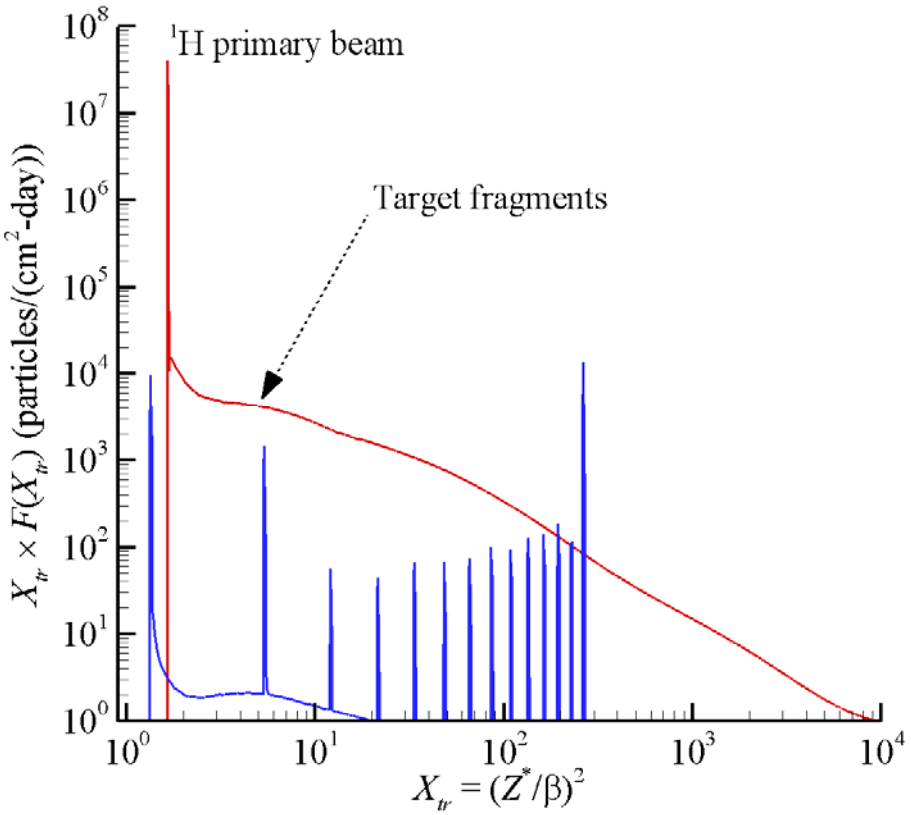

- The ^{1}H beam (560 MeV) spectrum is superimposed on the ^{28}Si results
- The final spectrum is the superposition of all discrete beam results

Beam Specification Strategy

- Track structure parameter, $X_{tr} = (Z^*/\beta)^2$, has been presented as an improved descriptor of track structure effects compared to LET alone [5]
- Beam selection not guided by X_{tr} spectra, so $F(X_{tr})$ provides somewhat of an independent check

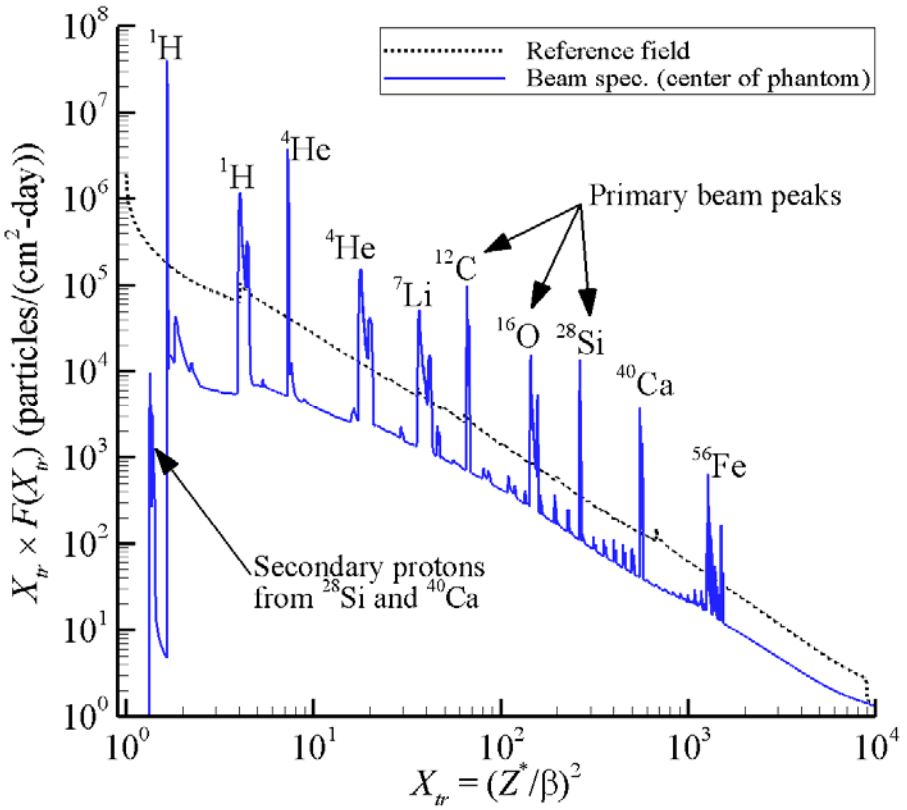

- Large peaks associated with primary beams
- Smaller peaks mainly attributed to heavy ion fragments with similar velocity as primary beam
  - Secondary proton peak from higher energy ^{28}Si and ^{40}Ca beams can be clearly seen

Beam Specification Strategy

- Track structure parameter, $X_{tr} = (Z^*/\beta)^2$, has been presented as an improved descriptor of track structure effects compared to LET alone [5]
- Beam selection not guided by X_{tr} spectra, so $F(X_{tr})$ provides somewhat of an independent check

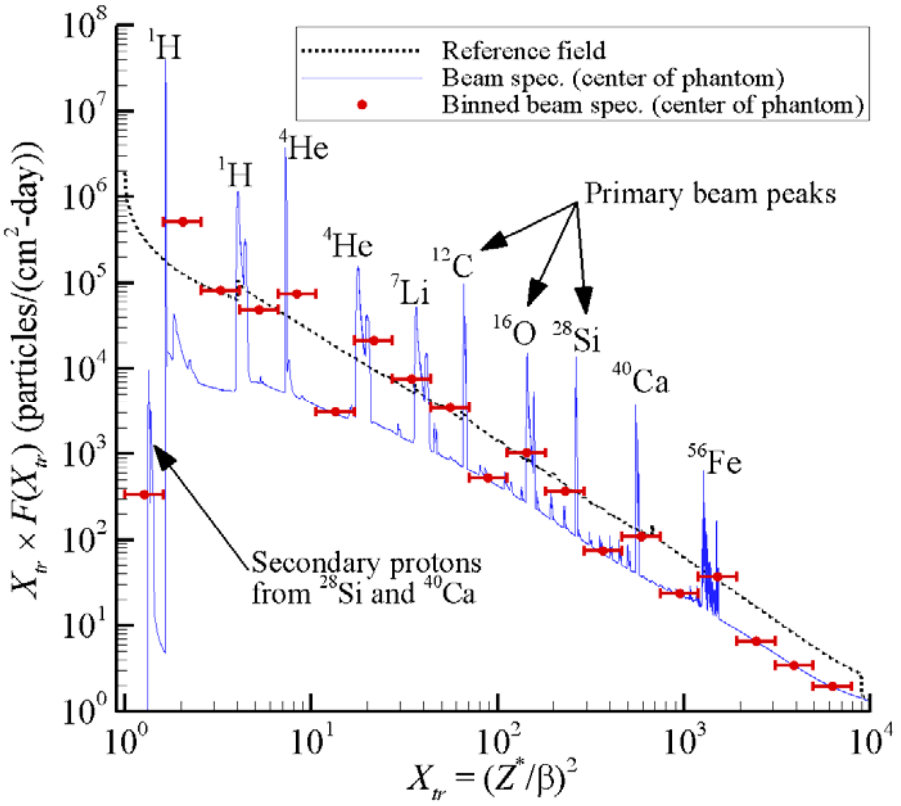

- In order to improve plot clarity, the $F(X_{tr})$ spectrum from the beams is binned to show general behavior

Beam Specification Strategy

- Track structure parameter, $X_{tr} = (Z^*/\beta)^2$, has been presented as an improved descriptor of track structure effects compared to LET alone [5]
- Beam selection not guided by X_{tr} spectra, so $F(X_{tr})$ provides somewhat of an independent check

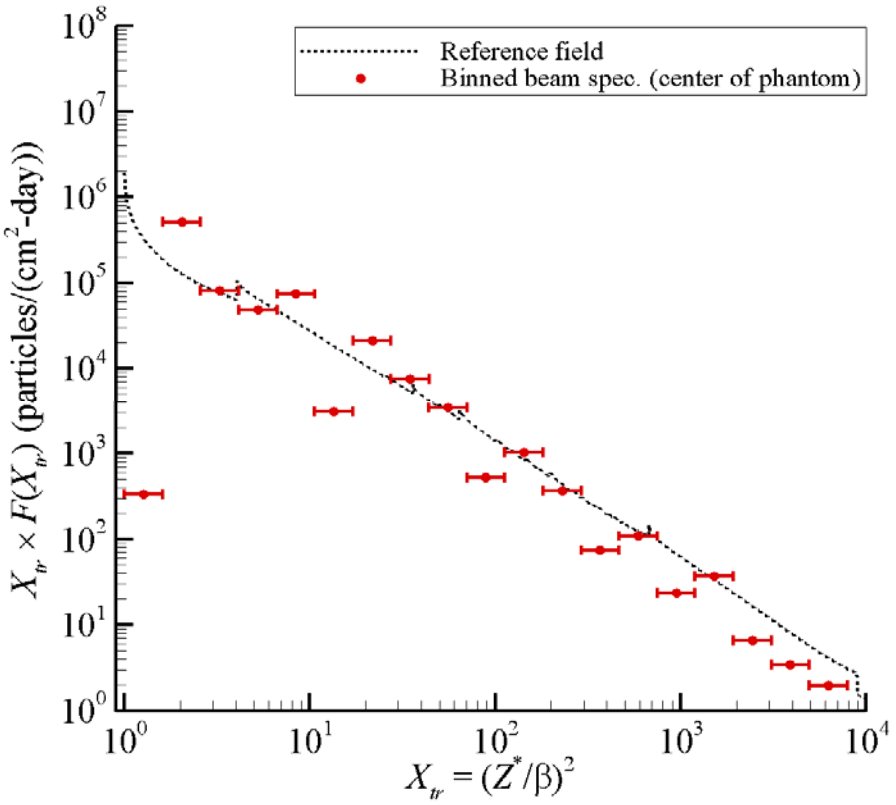

- Important to remember that beams were not selected to match this spectrum
- Given the relatively low number of beams, overall agreement is actually good

Beam Specification Strategy: Refinement

- The proposed strategy allows for systematic refinement by simply increasing the number of LET bins
- In this example, the LET domain is separated into 30 bins and the analysis is repeated
  - Internal phantom contours were examined and showed similar results as the 10 beam case
  - Improved agreement in spectral and integrated quantities can be seen

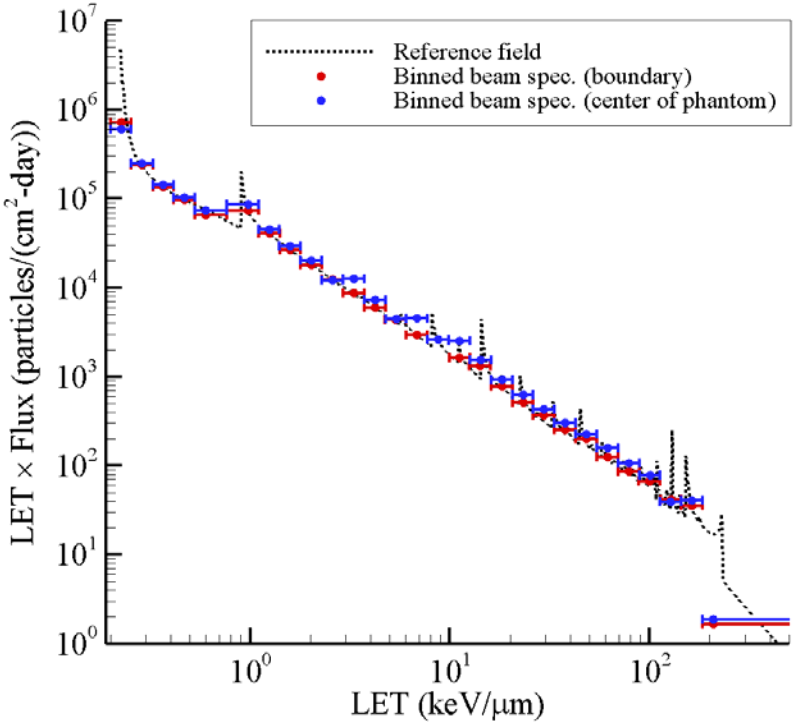

	D	H_{solid}	$\langle Q_{solid} \rangle$
Boundary	117.3	248.2	2.11
Center of phantom	131.5	326.7	2.48
Reference field (ions only)	117.3	298.2	2.54

Beam Specification Strategy: Refinement

- Improved agreement in track structure parameter spectra is seen
- Beam selection based only on LET spectrum appears to provide reasonable representation of the X_{tr} spectrum
- Improved agreement achieved with increased number of beams
- Optimization strategies could also be pursued to balance overall agreement between LET and X_{tr} spectra

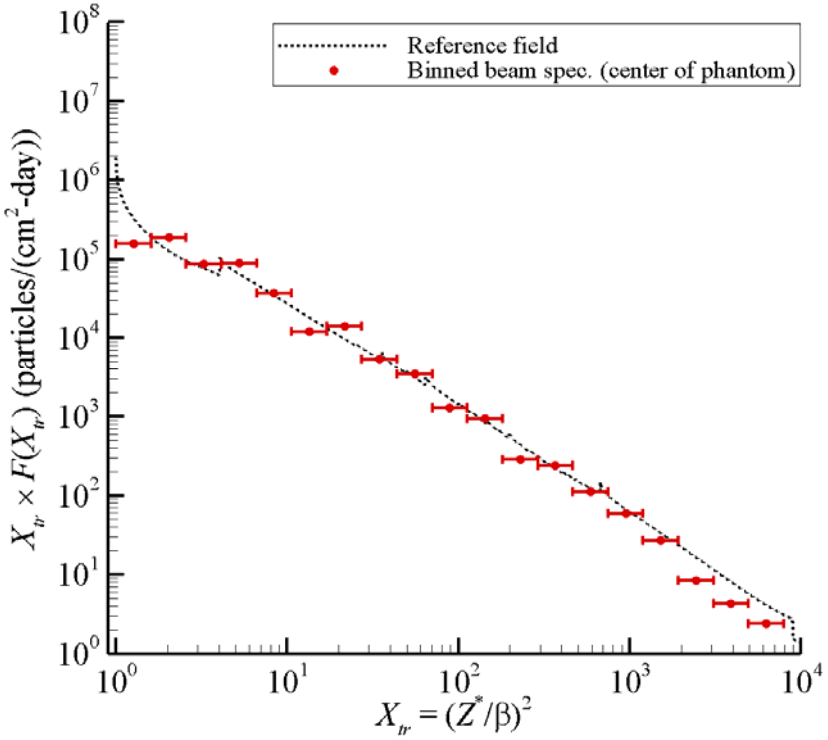

Discussion

- Proposed strategy for beam selection provides a systematic approach for reproducing the reference field LET spectrum and related quantities
  - Sensitivity analyses and energy constraints provide supplementary information
  - Integrated quantities such as a dose, dose eq., and <Q> well represented
  - Track structure spectrum reasonably well represented even though it wasn't targeted
  - Optimization strategies could be pursued to improve overall agreement across all quantities considered

- Proposed strategy does have some drawbacks
  - Track structure characteristics
  - Lower energy constraint associated with ion stoppage in animal model
  - Neutron and π/EM components

Discussion

- Track structure
  - Proposed strategy represents $F(X_{tr})$ spectrum reasonably well
  - Due to energy constraints, most beam energies were focused in the 200 MeV/n – 600 MeV/n range
  - Unclear if track structure characteristics of simulator will closely represent what might be expected in space
  - Especially important given ~half of the exposure is delivered by energies below 100 MeV/n

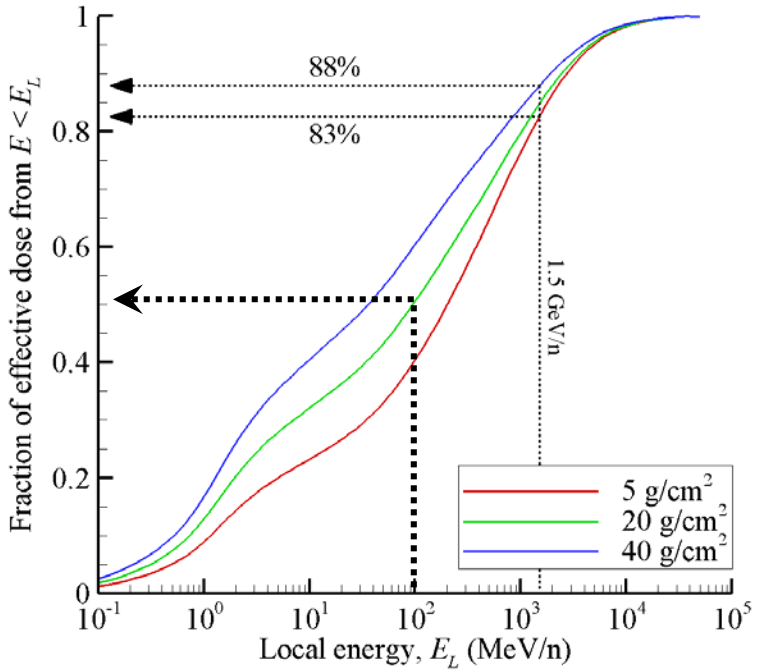

Discussion

- Lower energy constraint
  - Lower energy ions contribute significantly to exposure but are not explicitly included in simulator design
  - For cell cultures, the lower energy constraint could be relaxed
  - Proposed strategy could be modified to include a spectrum of low energy ions (degraders) but would require further analysis to integrate into the simulator design
  - Could leave design as-is and augment with increased complexity at a later date

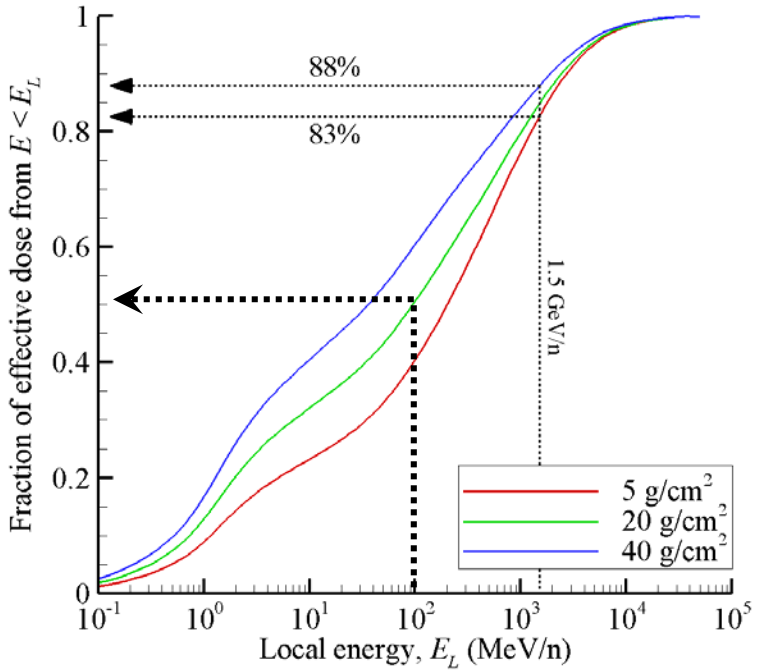

Discussion

- Neutrons
  - Neutron spectrum of reference field shown below
  - Neutron dose is defined here as energy deposited by heavy target fragments (Z > 2) produced in nuclear collisions (elastic recoil and inelastic products)
  - Most of the exposure comes from neutrons between 1 MeV and 1 GeV

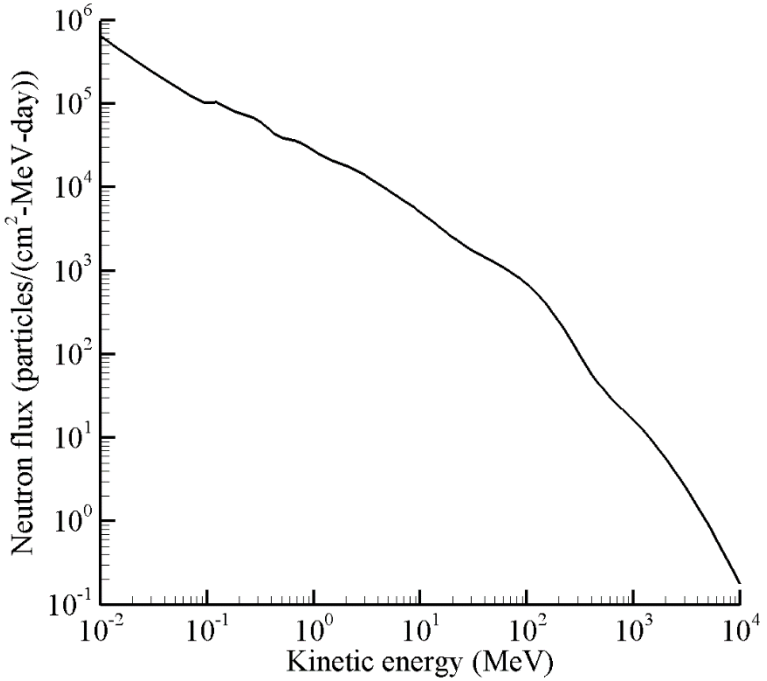

Discussion

- Neutron beam not currently available at NSRL
  - Even if it were, a pure neutron spectrum would induce a different exposure than what is defined presently
- Could represent heavy target fragment spectrum in some way, but might be difficult
  - Could use models to predict heavy target fragment spectrum (<10 MeV ions) and implement degraders to provide continuous spectrum
  - Could replace low energy target fragments with high energy ions with much higher Z value (i.e. same LET)
- Could also just ignore neutron component for now (and π/EM cascade)
  - Neutrons contribute small amount to dose and 7% to dose equivalent for reference environment
  - Likely this much error in any simulator design
  - Could again view the neutron and π/EM components as augmentations to the existing design to be added at a later date

Summary

- Current (and upgraded) facility constraints limit the ability to simulate the external, free space field directly
  - Proposed simulator design instead focuses on reproducing the local tissue field

- Variation in the induced tissue field was examined, and it was determined that a single reference environment for deep space is reasonable at this time

- An approach for beam selection in the simulator was presented
  - The approach is tied directly to the LET spectrum of the reference environment and allows systematic improvements to be made
  - Spectral quantities and integrated quantities are well represented
  - Optimization procedures could be developed to improve overall agreement across all quantities

- Drawbacks of the proposed strategy include
  - Possible lower energy constraints associated with animal models
  - Neutron and π/EM components
  - These drawbacks could be addressed by augmenting the existing design if necessary

References

[1] Slaba, T.C. and Blattnig, S.R., GCR environmental models III: GCR model validation and propagated uncertainties in effective dose. *Space Weather* **12**: 233-245, 2014.

[2] Slaba, T.C., Blattnig, S.R., Reddell, B., Bahadori, A., Norman, R.B., Badavi, F.F., Pion and electromagnetic contribution to dose: comparisons of HZETRN to Monte Carlo results and ISS data. *Adv. Space Res.* **52**: 62-78, 2013.

[3] Slaba, T.C., Blattnig, S.R., Badavi, F.F., Stoffle, N.N., Rutledge, R.D., Lee, K.T., Zapp, E.N., Dachev, Ts. P., Tomov, B.T., Statistical Validation of HZETRN as a Function of Vertical Cutoff Rigidity using ISS Measurements. *Adv. Space Res.* **47**: 600-610, 2011.

[4] Wilson, J.W., Tripathi, R.K., Mertens, C.J., Blattnig, S.R., Clowdsley, M.S., Verification and validation: High charge and energy (HZE) transport codes and future development. NASA TP-2005-213784, 2005.

[5] Cucinotta, F.A., Kim, M.Y., Chappell, L.J., Space radiation cancer risk projections and uncertainties – 2012. NASA TP 2013-207375, 2013.

[6] Walker, S.A., Clowdsley, M.S., Abston, H.L., Simon, M.A., Radiation exposure analysis supporting the development of solar particle event shielding technologies. 43rd International Conference on Environmental Systems, 2013.

[7] Simon, M.A., Cerro J.A., Latorella, K., Clowdsley, M., Watson, J., Albertson, C., Norman, R., Le Boffe, V., Walker, S., Design of two RadWorks storm shelters for solar particle event shielding. AIAA Space 2014 Conference and Exposition, 2014.

[8] O'Neill, P.M., Badhwar-O'Neill galactic cosmic ray flux model – revised. *IEEE Trans. Nuc. Sci.*, **57**: 3148–3153, 2010.

[9] Wilson, J.W., Townsend, L.W., Schimmerling, W., Khandelwal, G.S., Khan, F., Nealy, J.E., Cucinotta, F.A., Simonsen, L.C., Shinn, J.L., Norbury, J.W., Transport methods and interactions for space radiations, NASA RP-1257, 1991.

[10] Slaba, T.C., Blattnig, S.R., Badavi, F.F., Faster and more accurate transport procedures for HZETRN. *J. Comp. Phys.* **229**: 9397-9417, 2010.

[11] Slaba, T.C., Blattnig, S.R., Aghara, S.K., Townsend, L.W., Handler, T., Gabriel, T.A., Pinsky, L.S., Reddell, B., Coupled neutron transport for HZETRN. *Radiat. Meas.* **45**: 173-182, 2010.

[12] Norman, R.B., Blattnig, S.R., De Angelis, G., Badavi, F.F., Norbury, J.W., Deterministic pion and muon transport in Earth's atmosphere. *Adv. Space Res.* **50**: 146-155, 2012.

[13] Norman, R.B., Slaba, T.C., Blattnig, S.R., An extension of HZETRN for cosmic ray initiated electromagnetic cascades. *Adv. Space Res.* **51**: 2251-2260, 2013.

[14] Kramer, R., Vieira, J.W., Khoury, H.J., Lima, F.R.A., Loureiro, E.C.M., Lima, V.J.M., Hoff, G., All about FAX: A female adult voxel phantom for Monte Carlo calculations in radiation protection dosimetry. *Phys. Med. Biol.* **49**: 5203-5216, 2004.

[15] Badavi, F.F., Xapsos, M.A., Wilson, J.W., An analytical model for the prediction of a micro-dosimeter response function. *Adv. Space Res.* **44**: 190-201, 2009.

BACKUP: Variation in Local Field – Shielding

- Plots below show relative contribution to dose and dose equivalent for various charge groups
  - Protons and alphas account for more than half of the exposure
  - Breakup of HZE component can be clearly seen in breast dose equivalent
  - Relative contributions of particles types show some variation, but likely still within environmental and physics modeling uncertainty

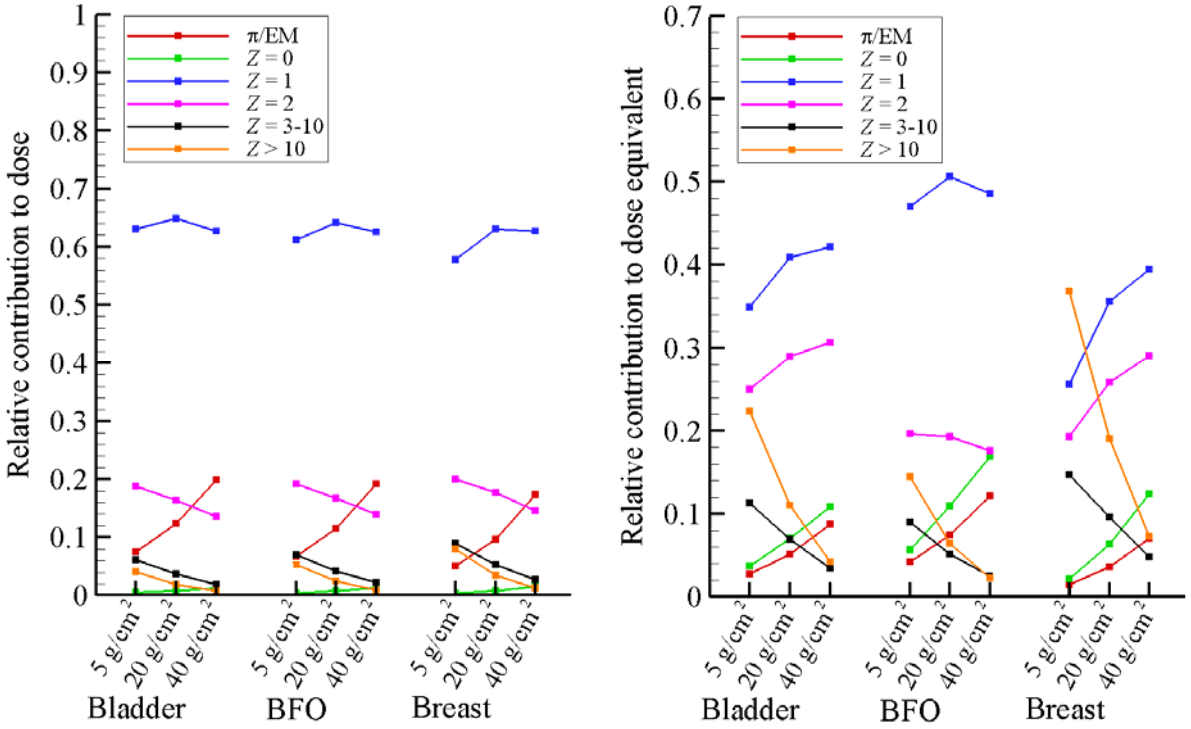

BACKUP: HZETRN beam transport

- The space radiation transport code HZETRN transports broad energy spectra through shielding materials
  - Numerical procedures have been heavily modified and improved in recent years
  - This allows relatively narrow spectra to be considered using a subtraction approach
  - Multiple scattering and straggling are not included in the computational procedure as they have been found to be less important in space applications
- Subtraction approach
  - Transport boundary condition A and compute quantities of interest
  - Transport boundary condition B and compute quantities of interest
  - Difference of results from A-B is identical to transporting boundary condition C directly
  - ε chosen to provide ±5% beam spread

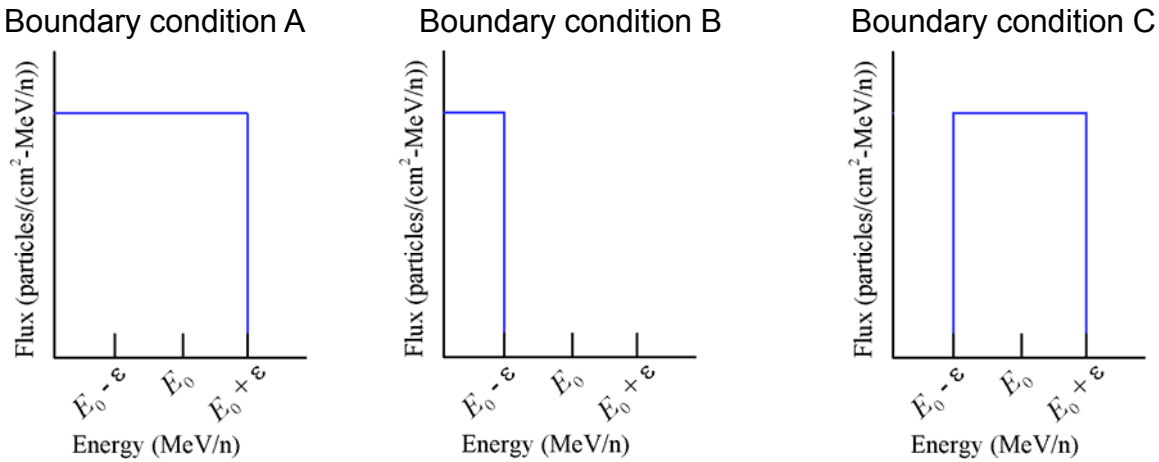

BACKUP: HZETRN beam validation

- Data below shows Bragg peak comparisons between HZETRN, Germ, and NSRL results
  - GERM transport uses 1D Monte Carlo transport with QMSFRG heavy ion physics

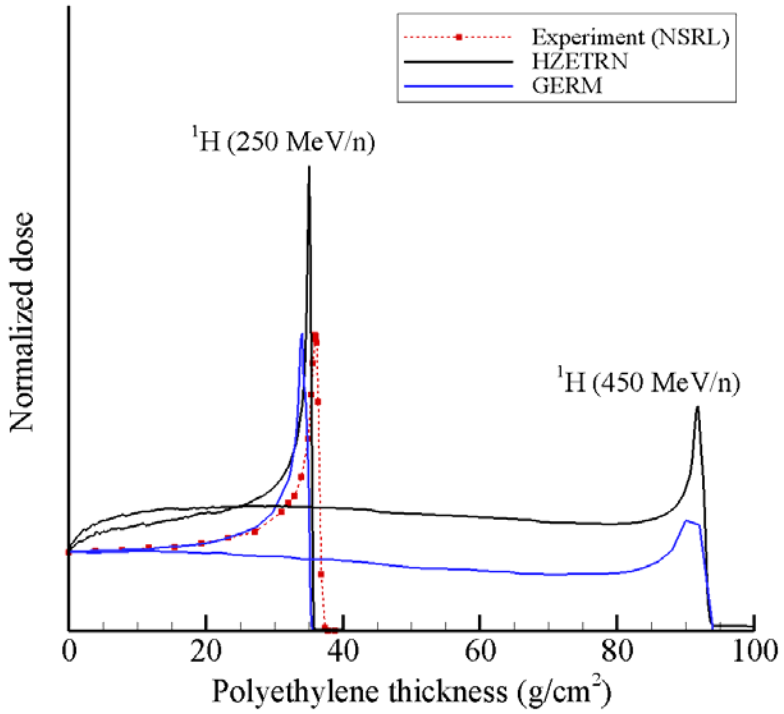

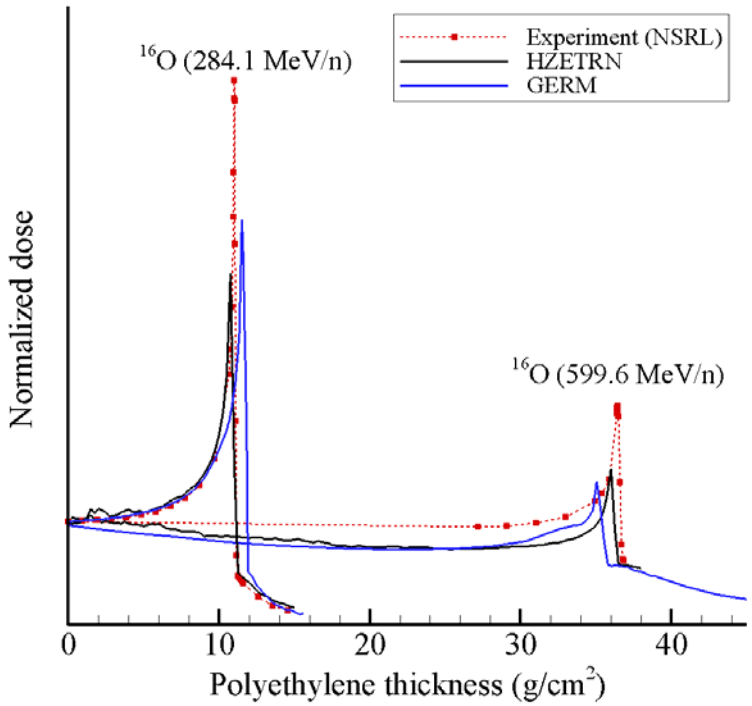

BACKUP: HZETRN beam validation

- Data below shows Bragg peak comparisons between HZETRN, Germ, and NSRL results
  - GERM transport uses 1D Monte Carlo transport with QMSFRG heavy ion physics

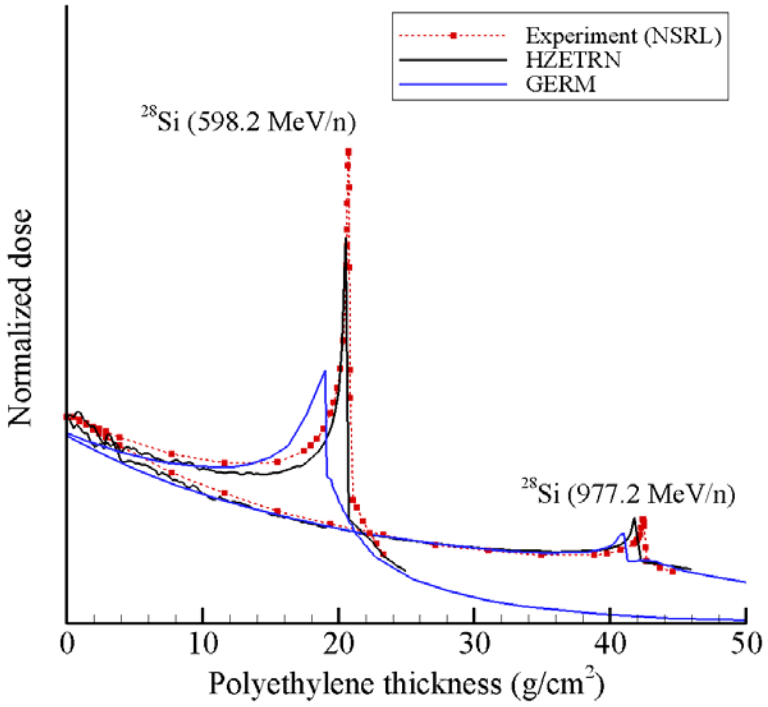

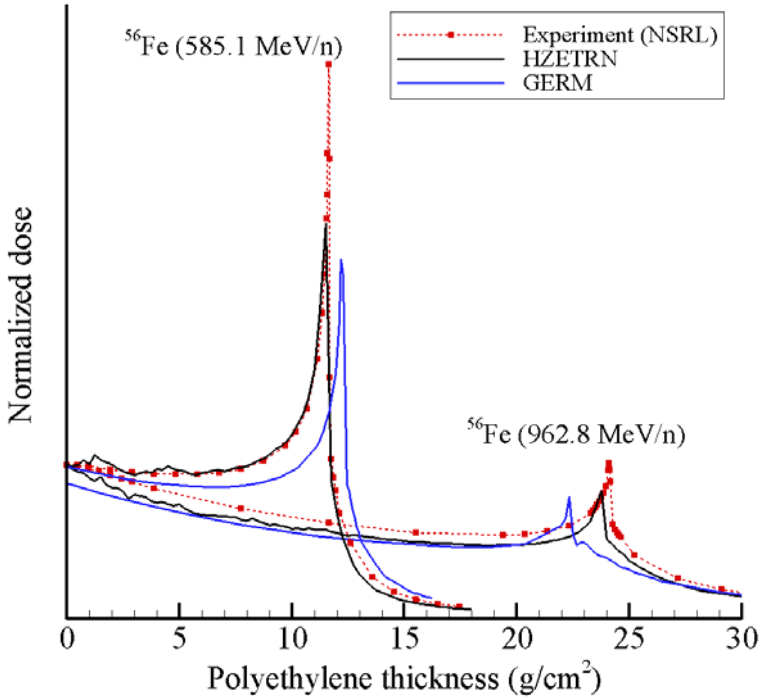

BACKUP: Simulate Free Space

- Comparisons are made between full reference environment and the BFO environment behind 20 g/cm^2 aluminum shielding during solar minimum with two different energy constraints applied to boundary condition
  - Energy constraint 1: Current NSRL limits – protons up to 2.5 GeV and heavier ions up to 1 GeV/n
  - Energy constraint 2: Upgrade NSRL limits – protons up to 4 GeV and heavier ions up to 1.5 GeV/n

- Results for energy constraint 1 are scaled by 1.85
- Results for energy constraint 2 are scaled by 1.49

- Table below compares dose and dose equivalent values

	D	H_{solid}	$\langle Q_{solid} \rangle$
Current NSRL constraints	72.2 (133.9)	170.8 (316.7)	2.4
Upgraded NSRL constraints	89.7 (133.9)	223.9 (333.7)	2.5
Reference field	133.9	336.6	2.5

Results in parentheses scaled by 1.85

Results in parentheses scaled by 1.49

BACKUP: Simulate Free Space

- Plots below compare LET and X_{tr} spectra of reference field to those obtained with boundary condition energy cutoffs
  - Scale factor of 1.85 applied to results using energy cutoff 1
  - Scale factor of 1.49 applied to results using energy cutoff 2

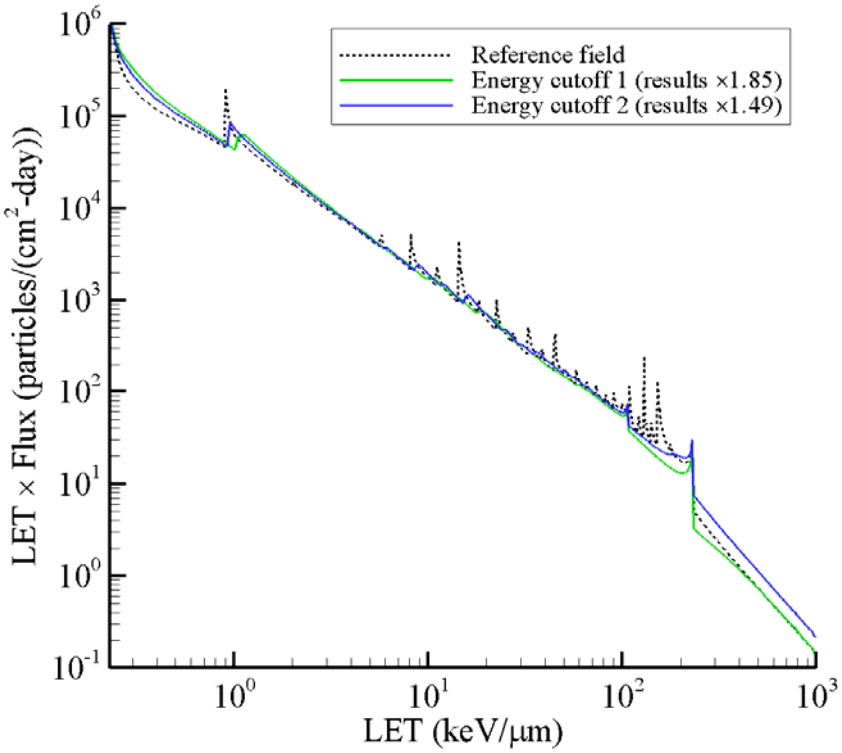

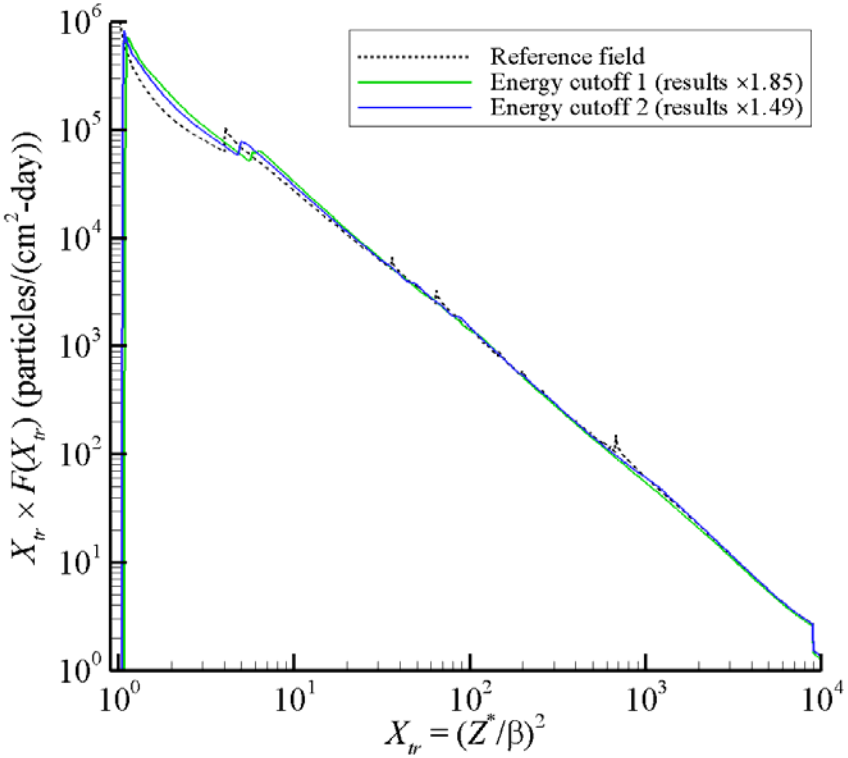

BACKUP: Simulate Free Space

- Plots below compare nucleon spectra of reference field to those obtained with boundary condition energy cutoffs
  - Scale factor of 1.85 applied to results using energy cutoff 1
  - Scale factor of 1.49 applied to results using energy cutoff 2

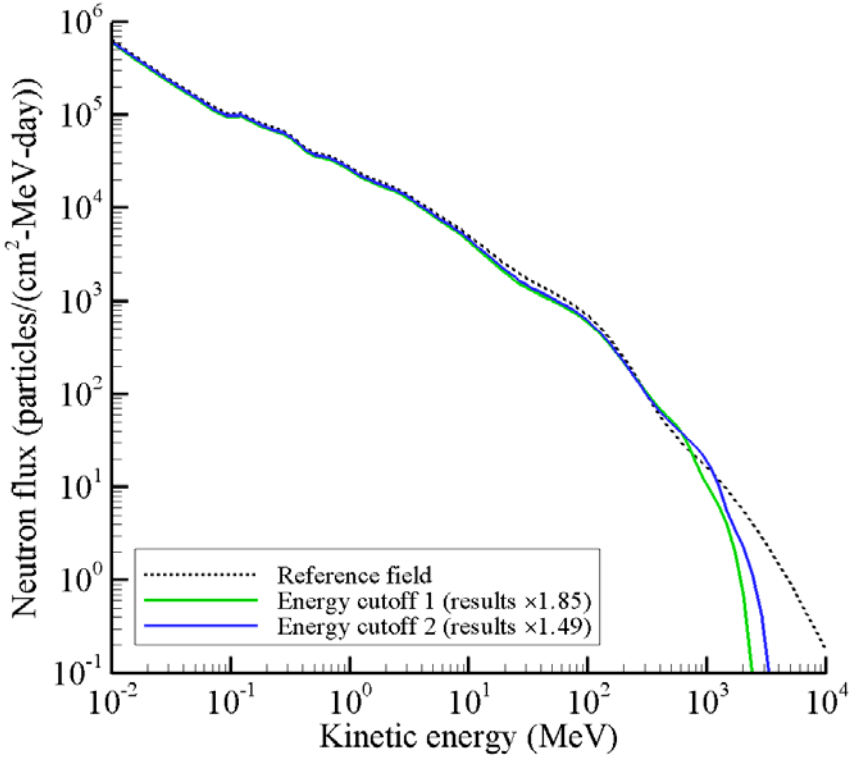

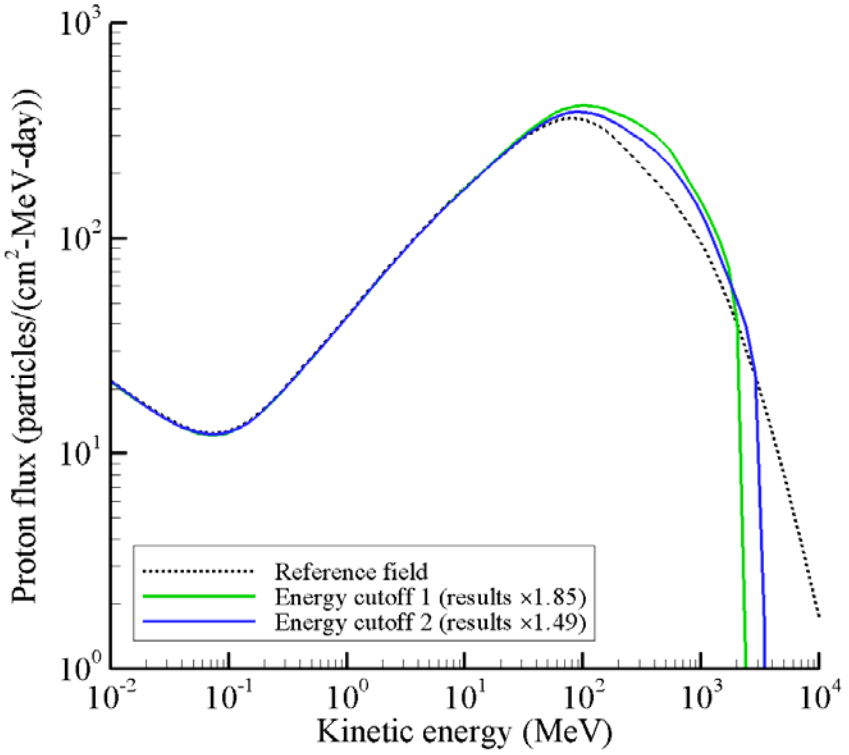

BACKUP: LET and X_{tr} spectra

- LET spectrum is computed from flux

$$\frac{d\phi(L)}{dL} = \sum_Z \frac{d\phi(Z,E)}{dE}\left|\frac{dE}{dL}\right| = \sum_Z \frac{d\phi(Z,E)}{dE}\left|\frac{dL}{dE}\right|^{-1}$$

- X_{tr} spectrum is computed from flux

$$\frac{d\phi(X_{tr})}{dX_{tr}} = \sum_Z \frac{d\phi(Z,E)}{dE}\left|\frac{dE}{dX_{tr}}\right| = \sum_Z \frac{d\phi(Z,E)}{dE}\left|\frac{dX_{tr}}{dE}\right|^{-1}$$

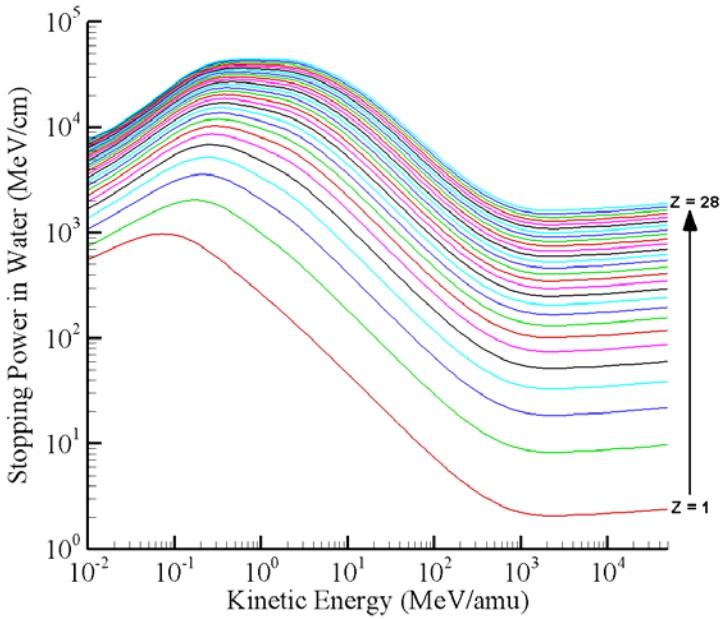

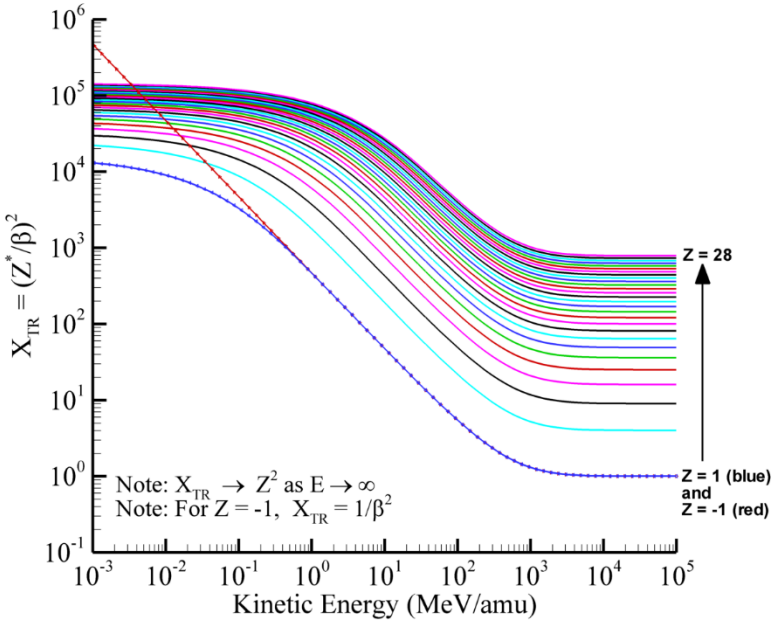

BACKUP: DH fraction vs. depth

- Plots below show relative contributions to dose and dose equivalent versus aluminum shielding thickness during solar min
  - Z ≤ 2 includes neutrons, light ions, and π/EM

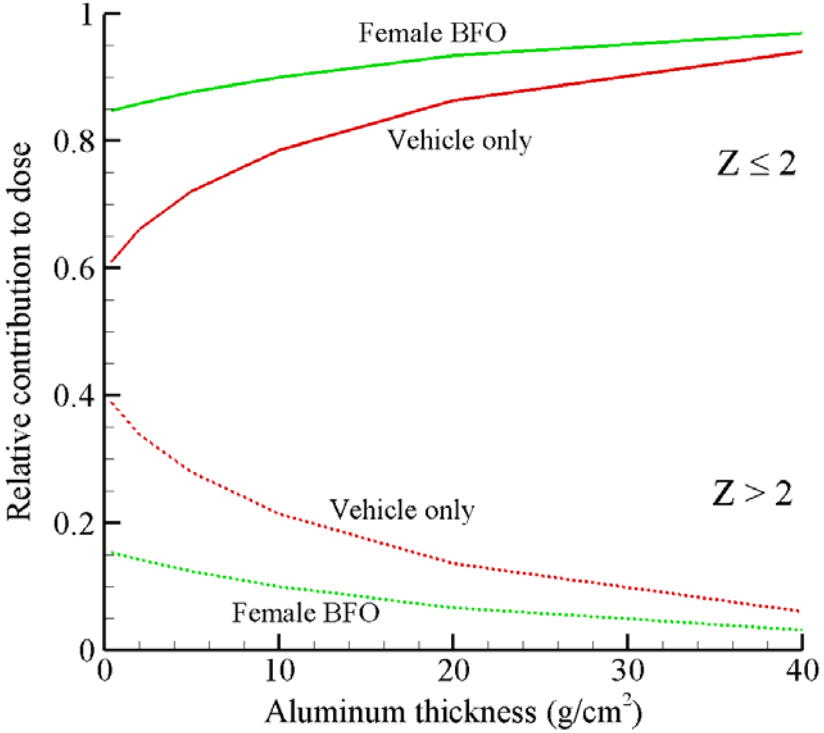

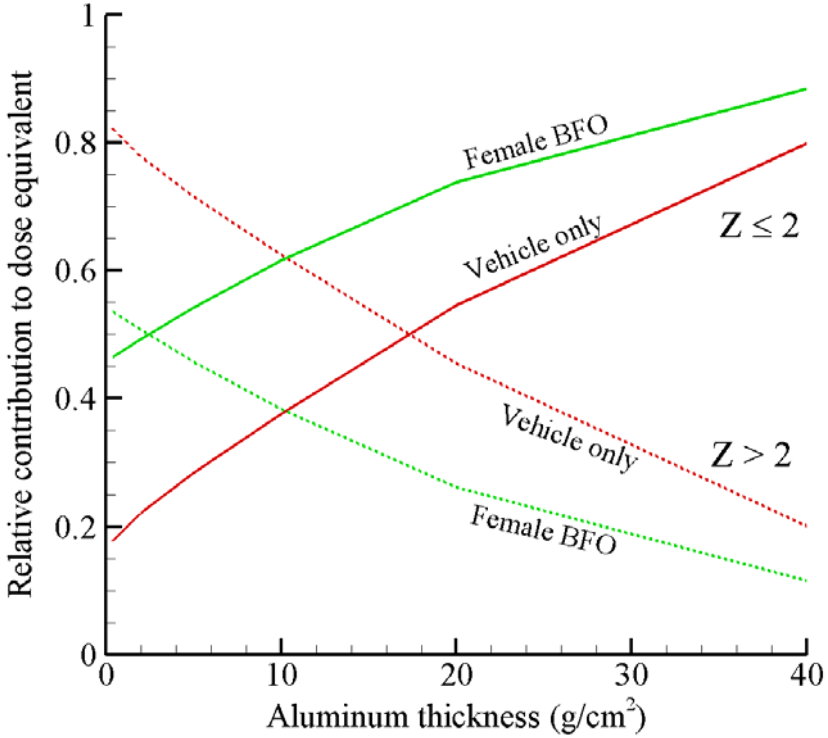

BACKUP: Rotation Images

- Results below assume full reference field is being simulated
- Some variation within mouse will occur at static positions
  - Greatest variation occurs when mouse is aligned with beam axis (~±15%)

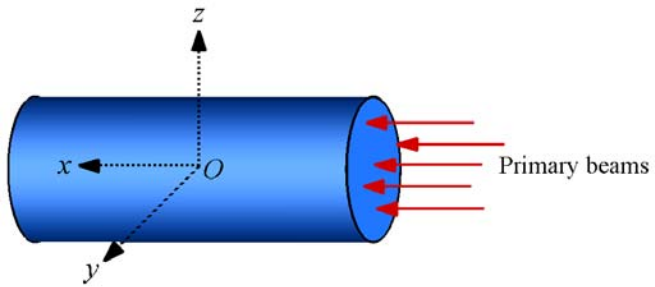

Rotations taken about
z-axis in *xy*-plane